The Plant Journal (2007) **52**, 263–285 doi: 10.1111/j.1365-313X.2007.03233.x

Molecular phenotyping of lignin-modified tobacco reveals associated changes in cell-wall metabolism, primary metabolism, stress metabolism and photorespiration

Rebecca Dauwe[1,2,†], Kris Morreel[1,2], Geert Goeminne[1,2], Birgit Gielen[3], Antje Rohde[1,2], Jos Van Beeumen[4], John Ralph[5], Alain-Michel Boudet[6], Joachim Kopka[7], Soizic F. Rochange[6], Claire Halpin[8], Eric Messens[1,2] and Wout Boerjan[1,2,*]

[1]*Department of Plant Systems Biology, Flanders Institute for Biotechnology, Technologiepark 927, 9052 Gent, Belgium,*
[2]*Department of Molecular Genetics, Ghent University, Technologiepark 927, 9052 Gent, Belgium,*
[3]*Department of Biology, University of Antwerp, Universiteitsplein 1, 2610 Wilrijk, Belgium,*
[4]*Department of Biochemistry, Physiology and Microbiology, Ghent University, K.L. Ledeganckstraat 35, 9000 Gent, Belgium,*
[5]*US Dairy Forage Research Center, USDA–Agricultural Research Service and Department of Biological Systems Engineering, University of Wisconsin-Madison, Madison, Wisconsin 53706-1108, USA,*
[6]*Surfaces Cellulaires et Signalisation chez les Végétaux, Centre National de la Recherche Scientifique-Université Paul Sabatier, Unité Mixte de Recherche 5546, Pôle de Biotechnologie Végétale, 24 chemin de Borderouge, BP 42617, 31326 Castanet, France,*
[7]*Max-Planck Institute of Molecular Plant Physiology, Cooperative Research Group, Am Mühlenberg 1, 14476 Golm, Germany, and*
[8]*University of Dundee, Plant Research Unit at the Scottish Research Institute, Invergowrie, Dundee DD2 5DA, UK*

Received 14 March 2007; revised 16 May 2007; accepted 12 June 2007.
[*]For correspondence (fax +32 9 3313809; e-mail wout.boerjan@psb.ugent.be).
[†]Present address: Wood Science Department, The University of British Columbia, Vancouver, BC V6T 1Z4, Canada.

Summary

Lignin is an important component of secondarily thickened cell walls. Cinnamoyl CoA reductase (CCR) and cinnamyl alcohol dehydrogenase (CAD) are two key enzymes that catalyse the penultimate and last steps in the biosynthesis of the monolignols. Downregulation of CCR in tobacco (*Nicotiana tabacum*) has been shown to reduce lignin content, whereas lignin in tobacco downregulated for CAD incorporates more aldehydes. We show that altering the expression of either or both genes in tobacco has far-reaching consequences on the transcriptome and metabolome. cDNA-amplified fragment length polymorphism-based transcript profiling, combined with HPLC and GC–MS-based metabolite profiling, revealed differential transcripts and metabolites within monolignol biosynthesis, as well as a substantial network of interactions between monolignol and other metabolic pathways. In general, in all transgenic lines, the phenylpropanoid biosynthetic pathway was downregulated, whereas starch mobilization was upregulated. CCR-downregulated lines were characterized by changes at the level of detoxification and carbohydrate metabolism, whereas the molecular phenotype of CAD-downregulated tobacco was enriched in transcript of light- and cell-wall-related genes. In addition, the transcript and metabolite data suggested photo-oxidative stress and increased photorespiration, mainly in the CCR-downregulated lines. These predicted effects on the photosynthetic apparatus were subsequently confirmed physiologically by fluorescence and gas-exchange measurements. Our data provide a molecular picture of a plant's response to altered monolignol biosynthesis.

Keywords: metabolomics, transcriptomics, CCR, CAD, oligolignol.

Introduction

Lignin is an aromatic heteropolymer that is mainly present in the walls of secondarily thickened cells (Boerjan *et al.*, 2003; Ralph *et al.*, 2004). It is generated from the oxidative polymerization of monolignols, and makes the wall rigid and hydrophobic, allowing transport of water and solutes through the vascular system. In addition to its structural role

in the vascular tissues, lignin also protects plants against invading pathogens. The lignin biosynthetic pathway has attracted significant research attention because lignin is a limiting factor in a number of agro-industrial processes, such as chemical pulping, forage digestibility, and the processing of lignocellulosic plant biomass to bioethanol (Baucher *et al.*, 2003; US Department of Energy, 2006). Consequently, most of the genes involved in the monolignol biosynthetic pathway have been cloned and their function assigned through genetic modification and the characterization of mutants (Boerjan *et al.*, 2003). Although analyses of the consequences of altering the expression of these genes have mostly been restricted to the study of lignin amount and composition, more recent transcript profiling of *Arabidopsis thaliana pal*, *cad* and *c3h* mutants, maize (*Zea mays*) *bm3* mutants, and antisense *4CL1* and *F5H*-overexpressing aspen (*Populus* sp.) indicates far-reaching consequences of the mutations on various pathways (Abdulrazzak *et al.*, 2006; Ranjan *et al.*, 2004; Robinson *et al.*, 2005; Rohde *et al.*, 2004; Shi *et al.*, 2006; Sibout *et al.*, 2005). Hence, it is conceivable that the observed effects on the cell wall in transgenic plants with altered monolignol biosynthesis are not merely due to the reduced flux through the altered biosynthetic step, but are the combined outcome of a much more complex interplay of various metabolic pathways. In addition, adverse effects on plant growth in lignin-modified plants may be caused by secondary effects, rather than defects in lignin biosynthesis *per se*. Indeed, some transgenic tobacco (*Nicotiana tabacum*) lines with reduction in lignin amount have growth defects, whereas other lines with comparable reductions develop normally (Chabannes *et al.*, 2001a,b). In Arabidopsis, it has been shown that growth defects in *hct* mutants are attributable to elevated flavonoid levels (Besseau *et al.*, 2007). Understanding the molecular mechanisms that plants use to respond to cell-wall defects is essential in order to design plant cell walls with improved properties without compromising plant health and viability (Möller, 2006).

The last two steps in the biosynthetic pathway of the monolignols are catalysed by cinnamoyl CoA reductase (CCR) and cinnamyl alcohol dehydrogenase (CAD). In tobacco, only one cDNA has been identified so far for *CCR* (O'Connell *et al.*, 2002; Piquemal *et al.*, 1998) and two for *CAD* (Knight *et al.*, 1992). The two *CAD* cDNA sequences show strong homology both in the coding region (94%) and in the 5′ and 3′ untranslated regions (88% and 82%, respectively), supporting the hypothesis that these genes are derived from the two ancestral species, *N. sylvestris* and *N. tomentosiformis*, rather than representing two distinct *CAD* genes. Transgenic tobacco plants downregulated for the corresponding genes have already been thoroughly characterized for alterations in morphology, lignin amount and composition, and cell-wall structure (Chabannes *et al.*, 2001a,b; Halpin *et al.*, 1994; O'Connell *et al.*, 2002; Piquemal *et al.*, 1998; Ralph *et al.*, 1998). Downregulation of CCR in tobacco results in reduced lignin content. Lignin in these plants is characterized by a reduced incorporation of cinnamaldehydes and elevated levels of ferulate and tyramine ferulate. Xylem vessels are collapsed, leaves are dark-green and wrinkled, and, in addition, strongly downregulated lines are smaller in size with yellowish areas between the leaf veins. Tobacco plants downregulated for CAD have higher cinnamaldehyde levels in lignin, but normal lignin content and overall plant appearance. Double transformants with reductions in the expression of both *CCR* and *CAD* have less lignin but no collapsed vessels. All three types of transgenic lines have a reddish-colored xylem, attributable to the presence of unusual phenolics during lignin polymerization. Because these lines are so well characterized, they are ideal models to study how the various phenotypes are elaborated at the molecular level and how plants respond to cell-wall defects. Here, we analysed the transcriptome and metabolome of these transgenic lines. Our data show that, depending on the modified step, alteration of monolignol biosynthesis can affect the transcript levels of other monolignol biosynthesis genes, and additionally those of starch and hemicellulose metabolism, respiration, photorespiration and stress pathways. The suggested effects of lignin modification on photorespiration and oxidative stress were further corroborated by physiological measurements. Together, our combined transcript and metabolite data reveal how monolignol and cell-wall biosynthesis are integrated into general metabolism, and show that perturbations of such processes are sensed and partially compensated for by plants.

Results

Comparative cDNA-AFLP profiling of xylem from CCR, CAD and double downregulated tobacco

cDNA-amplified fragment length polymorphism (AFLP)-based transcript profiling was performed on two pools of scraped xylem tissue, derived from wild-type tobacco (WT) and transgenic tobacco deficient in CCR (asCCR), CAD (asCAD) or both (DT) (Figure 1). Both single and double transformants developed normally and were hemizygous for the antisense constructs. Gene expression was surveyed with 189 primer combinations, yielding a total of approximately 11 000 transcript-derived fragments (TDFs) ranging from 50 to 500 bp. To determine the TDFs that accumulated differentially between the lines (dTDFs), the cDNA-AFLP gels were analysed by a combination of visual scoring and statistical analyses; 365 non-redundant bands had a significantly altered intensity in one or more transgenic lines, 186 of which were proven, after excision, re-amplification and sequencing, to represent a single transcript (Table 1; Tables S1 and S2). All further analyses were based on this set of 186 dTDFs.

Overall, a relatively stronger effect on the transcriptome was seen in asCCR (145 dTDFs) and in DT (131 dTDFs)

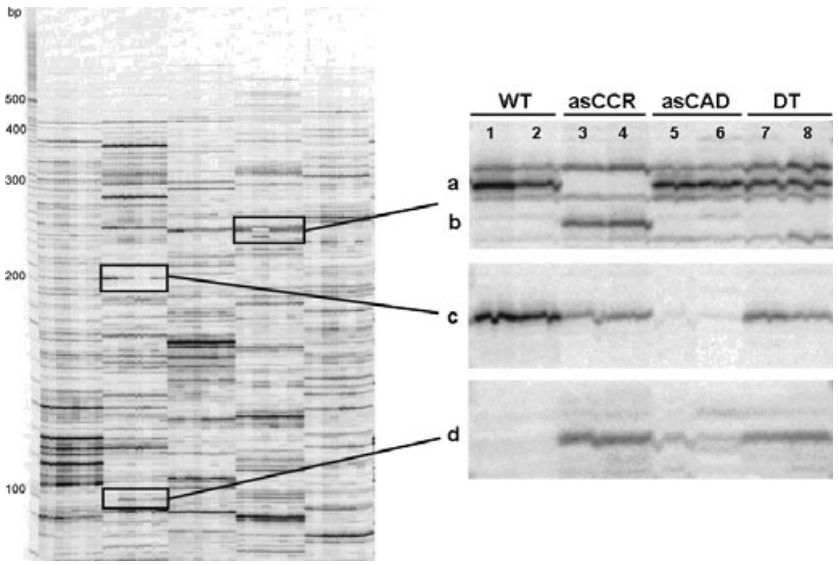

Figure 1. cDNA-AFLP transcript profiling of WT, asCCR, asCAD and DT tobacco xylem.
A typical cDNA-AFLP gel is shown. Amplification was performed with BstYIT + 2 and MseI + 1 primers. Gel sections containing dTDFs (a, b, c, d) that have been excised and re-amplified are enlarged. Two pools (lanes 1–8) are presented for each profile.

compared to asCAD (110 dTDFs; Figure 2a). All genes for which the transcript level was either upregulated in both asCCR and asCAD, or downregulated in both, also displayed the same change in transcript level in DT. For a set of 20 dTDFs, the accumulation was affected in the opposite way in asCCR and DT compared with asCAD. Only six dTDFs accumulated differentially in DT alone.

Based on sequence homology, 53% (98 dTDFs) of the 186 dTDFs were assigned a putative function, 14% (26 dTDFs) were similar to genes without known function, and for 33% (62 dTDFs), no hit with any sequence was found. Functional classification of the dTDFs (Table 1; Tables S1 and S2) indicated that transcript levels of genes involved in many aspects of both primary and secondary metabolism were affected, and hence that the effect of deficiency in one or both monolignol biosynthesis genes was not restricted to the phenylpropanoid biosynthetic pathway.

Correlation between expression patterns and function of the differentially expressed genes

Using hierarchical clustering, the dTDFs were divided into groups that had similar accumulation patterns across the various transgenic lines, and functional relationships between members of each group were examined (Figure S1). Of all 186 dTDFs, 59% could be divided into five main groups, each consisting of at least 18 dTDFs with highly similar accumulation patterns; the remaining 41% had no such patterns.

Group 1 (30 dTDFs) is the largest, and contains genes that were upregulated similarly in asCCR and in DT but were not or only modestly differentially regulated in asCAD. In this group, nine out of 13 dTDFs with known function belong to the detoxification class, eight of which represent glutathione *S*-transferases (GSTs) of at least two different types (including six dTDFs for the auxin-regulated GST, parA) and one dTDF that originates from an ABC transporter gene. Group 1 also contains a dTDF that corresponds to 3-phosphoglycerate (PGA) kinase, which is active centrally in carbon metabolism.

Group 2 (20 dTDFs) consists of genes that were mainly strongly upregulated in asCAD, including several light-related dTDFs [three dTDFs for chlorophyll *a/b*-binding protein (*CAB*), one for the phytochrome gene member *PHYA*, and one for late elongated hypocotyl (*LHY*)]. Several cell-wall-related dTDFs, corresponding to proteins involved in cell-wall expansion [expansin, lipid transfer protein (LTP), polygalacturonase (PGase), extensin] are found in this group, as well as two dTDFs corresponding to the same leucine-rich repeat receptor-like protein kinase (LRR-RLK) of unknown function.

Group 3 (22 dTDFs) comprises genes that were similarly downregulated in all transgenic lines. Half of the dTDFs to which a function could be assigned are involved in secondary metabolism [phenylalanine ammonia lyase (*PAL*), 4-coumarate:CoA ligase (*4CL*), caffeic acid *O*-methyltransferase (*COMT*) (two fragments), *CAD* and dihydroflavonol 4-reductase (*DFR*)]. The *PAL* dTDF is identical to a completely conserved region present in the three known tobacco *PAL* sequences (Fukasawa-Akada *et al.*, 1996; Nagai *et al.*, 1994; Pellegrini *et al.*, 1994). For the Arabidopsis homologues that are most closely related to these tobacco *PAL* sequences, *AtPAL1* and *AtPAL2*, a role in lignification has been demonstrated (Rohde *et al.*, 2004). The *4CL* dTDF aligns with a conserved region in the three available *4CL*-coding sequences from tobacco (Lee and Douglas, 1996) but the sequence is not identical (78.6% identity at the amino

Table 1 Identities, expression patterns and functional classification of the dTDFs isolated by cDNA-AFLP transcript profiling of WT, asCCR, asCAD and DT tobacco

			Mean band intensity				Arabidopsis closest homologue	
dTDF	Best hit	Description	WT	asCCR	asCAD	DT	AGI	E-value (BLASTP)
1 Metabolism, 18 entries (9.7%)								
1.1 Amino acid metabolism, six entries (3.2%)								
C32M4_019	spt:Q94BP8	Putative alanine aminotransferase (fragment), ACC synthase	435	441	*77**	411	At1g17290.1	0
C34M4_038	spt:Q83JW4	Hypothetical protein csdA, Aminotransferase, class V	6019	*976**	5969	*1085**	At1g08490.1	E-80
C33M2_033	sp:P38561	Glutamine synthetase root isozyme 3 (GS1-3)	1312	**5156***	1340	1247	At5g37600.1	0
T31M24_034	sp:P54767	Glutamate decarboxylase	6076	*1707**	*2111**	*1383**	At5g17330.1	0
C13M3_009	spt:Q9ZUY3	Putative chorismate mutase/ prephenate dehydratase	418	*168**	*121**	*132**	At2g27820.1	0
T41M13_010	spt:Q6FA02	Phospho-2-dehydro-3-deoxyheptonate aldolase/ 3-deoxy-D-arabino-heptulosonate-7-phosphate synthase	70	**246***	**300***	**307***	No hit	
1.2 C-compound and carbohydrate metabolism, eight entries (4.3%)								
T34M13_024	sp:Q42962	Phosphoglycerate kinase, cytosolic	257	**1681***	254	**1671***	At1g79550.2	0
T44M3_100	spt:Q9AXL6	β-glucosidase (fragment)	2526	749*	2528	*761**	At1g02850.2	E-147
T24M3_013	spt:Q9XH69	β-amylase (fragment)	253	**1660***	**1057***	**3281***	At5g18670.1	E-170
T23M2_052	spt:Q9FKY9	Pectinesterase like protein	1319	*620**	**2960***	*577**	At5g66920.1	0
T44M4_020	spt:Q40161	Polygalacturonase isoenzyme 1 β subunit (precursor)	213	137	**644***	151	At1g70370.1	0
C32M21_045	spt:Q6IVK7	Putative UDP-glucose dehydrogenase 1	12 527	*7486**	**16 798***	*9135**	At5g15490.1	0
C42M33_004	spt:Q6IVK6	Putative UDP-glucose dehydrogenase 2	1122	*486**	1264	*462**	At5g15490.1	0
C22M4_007	spt:Q9STB3	ADP-glucose pyrophosphorylase (fragment)	2241	*306**	*545**	*107**	At2g21590.1	0
1.3 Lipid, fatty acid and isoprenoid metabolism, three entries (1.6%)								
C32M3_007	spt:Q89R91	Epoxide hydrolase	347	*129**	**498***	*161**	At4g02340.1	E-44
C12M4_227	spt:Q8VY26	Hypothetical protein At4g32810, related to neoxanthin cleavage enzyme	2591	**13 964***	3237	**7883***	At4g32810.1	0
T22M1_092	spt:Q9SP65	1-deoxy-D-xylulose 5-phosphate synthase	8459	6334	6627	*2671**	At4g15560.1	0
1.4 Secondary metabolism, nine entries (4.8%)								
C12M12_025	spt:Q9SDZ2	2′-hydroxy isoflavone/dihydroflavonol reductase homologue (fragment) DFR1	1933	*205**	*75**	*224**	At2g45400.1	7.00E-83
T34M12_050	spt:Q42958	Caffeic acid *O*-methyltransferase OMT I	4817	*783**	*1180**	*1463**	At5g54160.1	E-160
T34M11_054	spt:Q42958	Caffeic acid *O*-methyltransferase OMT I	10 752	*5020**	*4218**	*4177**	At5g54160.1	E-160
T11M1_040	spt:Q9SDU0	4-coumarate:CoA ligase (fragment)	86 556	*43 484**	*18 239**	*54 693**	At4g19010.1	2.00E-45
T33M4_015	spt:Q9FSC7	Cinnamyl alcohol dehydrogenase	326	*117**	*80**	*75**	At3g19450.1	E-168
T12M3_027	spt:Q8H6 W0	Phenylalanine ammonia lyase 1	140	**1393***	**502***	**2000***	At3g53260.1	0
T43M1_043	spt:Q8H6 V6	Phenylalanine ammonia lyase	340	*162**	*86**	*80**	At3g53260.1	0
T21M21_028	spt:Q925P9	Adenosine kinase (fragment)	5098	3546	**8920***	4209	At3g09820.2	2.00E-11
C42M3_003	sp:Q9SF85	Adenosine kinase 1	4830	*2659**	**6371***	*2905**	At3g09820.1	0

Table 1 (Continued)

dTDF	Best hit	Description	Mean band intensity WT	asCCR	asCAD	DT	Arabidopsis closest homologue AGI	E-value (BLASTP)
2 Transcription, eight entries (4.3%)								
2.1 mRNA transcription, eight entries (4.3%)								
T34M12_054	sp:P06269	RNA polymerase α subunit	1393	**18 329***	2110	1876	No hit	
C32M23_005	spt:Q9FZ15	Tuber-specific and sucrose-responsive element binding factor, Myb-like transcription factor	2670	*1314**	3750	*233**	At5g67300.1	7.00E-79
C34M4_005	spt:O22230	Putative heat shock transcription factor	1832	*562**	*586**	*436**	At2g41690.1	E-144
C42M2_031	spt:Q9FEL0	AP2 domain-containing transcription factor (fragment)	2095	*767**	*1145**	*862**	At3g16770.1	4.00E-37
T21M14_041	spt:Q84UB0	Transcription factor Myb1	1759	1449	*470**	*560**	At1g19000.2	4.00E-57
T21M2_040	spt:Q8S9H7	MYB-like transcription factor DIVARICATA	101	**444***	82	**224***	At5g58900.1	4.00E-86
T41M3_003	spt:Q93YF1	Nucleic acid binding protein	149	**224***	126	**332***	At1g47490.1	E-142
T34M12_027	spt:Q8S249	Putative pumilio/Mpt5 family RNA-binding protein	2014	1897	*901**	2101	At2g29190.1	0
3 Protein synthesis,11 entries (5.9 %)								
3.1 Ribosome biogenesis, seven entries (3.8 %)								
T24M33_016	spt:Q9MAV9	Cytoplasmic ribosomal protein S13	530	624	**1704***	**894***	At3g60770.1	7.00E-80
T21M44_019	spt:Q8L6A3	Putative ribosomal protein L2 (fragment)	243	**2178***	229	189	At2g44065.2	8.00E-28
T21M23_022	spt:Q9ATF6	Ribosomal protein L17	1519	**3052***	*227**	1370	At3g04400.1	8.00E-77
T31M44_010	sp:P06379	Chloroplast 50S ribosomal protein L2	53	**1012***	73	59	At2g44065.2	2.00E-30
T11M4_025	spt:Q8S8 V3	Chloroplast 50S ribosomal protein L2	1808	**173 179***	1569	1594	At2g44065.2	2.00E-30
T11M1_026	spt:Q8S8 V3	Chloroplast 50S ribosomal protein L2	56 825	*4961**	55 897	68 607	At2g44065.2	2.00E-30
T23M1_023	sp:Q08069	40S ribosomal protein S8	246	**3498***	**1181***	**3227***	At5g20290.1	E-106
3.2 Translation, three entries (1.6%)								
T23M22_009	spt:O82278	Putative GTP-binding protein (this protein promotes the GTP-dependent translocation of the nascent protein chain from the A-site to the P-site of the ribosome)	646	*266**	631	*363**	At2g31060.1	0
C13M1_044	spt:Q9SQV1	Putative RNA helicase	459	**1221***	378	**1223***	At3g06480.1	0
C23M2_222	spt:Q9M9P8	T17B22.1 protein, helicase C, Rnase III	761	**15 211***	3163	**13 946***	At3g03300.1	0
3.3 Aminoacyl-tRNA synthetases, one entry (0.5 %)								
T31M2_015	sp:Q9KTX0	Histidyl-tRNA synthetase	166	**851***	**550***	**475***	At3g46100.1	8.00E-29
4 Protein fate (folding, modification, destination), eight entries (4.3%)								
4.1 Protein modification, one entry (0.5%)								
T21M24_045	sp:Q42539	Protein-L-isoaspartate *O*-methyltransferase	4571	**8016***	**8183***	**9368***	At3g48330.2	E-129
4.2 Proteolytic degradation, seven entries (3.8%)								
C41M1_050	spt:Q9SD67	FtsH metalloproteinase-like protein	206	**449***	*70**	**369***	At3g47060	0
C43M3_067	spt:Q9LM69	Hypothetical protein At1g20823, RING-type zinc finger	21 004	*9992**	18 520	*15 460**	At1g20823.1	E-111
T31M2_094	spt:Q9M7 K7	Ubiquitin protein ligase 2	1013	**2570***	905	**2420***	At1g55860.1	0
C12M2_018	spt:Q9M7 K6	E3 ubiquitin protein ligase UPL2	269	**678***	**604***	**767***	At1g70320.1	0
T24M32_013	spt:Q6K3D2	Putative F-box protein FBL2	633	**1098***	*122**	719	At3g58530.1	E-100
T41M11_031	spt:Q9SB64	Hypothetical protein At4g24690, ubiquitin-associated domain (UBA)-containing protein	1934	**5404***	**3179***	**5142***	At4g24690.1	0
C12M4_235	spt:O65493	Papain-type cysteine endopeptidase XCP1	5320	4085	**12 128***	4037	At4g35350	0

Table 1 (Continued)

dTDF	Best hit	Description	Mean band intensity				Arabidopsis closest homologue	
			WT	asCCR	asCAD	DT	AGI	E-value (BLASTP)
5 Cellular communication/signal transduction mechanism, 11 entries (6.0%)								
5.1 Transport facilities, three entries (1.6%)								
T41M2_008	sp:Q9SU64	Cyclic nucleotide- and calmodulin-regulated ion channel 16	1588	*285**	1556	*274**	At3g48010.1	0
T21M4_036	sp:O04289	Sulfate transporter 3.2	737	727	705	*185**	At4g02700.1	0
T24M12_002	spt:Q949 J9	Hypothetical protein, mechanosensitive ion channel	34	**259***	47	27	At1g58200.2	E-93
5.2 Intracellular signalling, four entries (2.2%)								
T13M1_078	spt:Q9SFE3	Putative phosphatidylinositol-4-phosphate 5-kinase	423	309	**1143***	536	At1g21920.1	0
T33M2_005	spt:Q942X2	Putative serine/threonine kinase PBS1 protein	164	**261***	129	**274***	At5g18610.1	0
T41M3_018	spt:Q8RWN3	Protein kinase-like protein	45	**56***	*25**	**65***	At3g25840.1	0
C43M2_033	spt:Q84TS1	Hypothetical protein OSJNBb0097 F01.10, PP2C-like	1161	**3958***	**1836***	**4093***	At2g46920.2	E-150
5.3 Transmembrane signal transduction, four entries (2.2%)								
C32M22_018	spt:O65238	T26D22.12 protein, B_lectin, serine/threonine protein kinase	314	328	230	**1093***	At5g35370.1	0
C32M21_016	spt:Q9FZP3	S-receptor kinase	185	**876***	*71**	*148**	At5g35370.1	0
C34M1_029	spt:Q9SSL9	Highly similar to receptor-like protein kinase	474	263	**3415***	387	At1g73080.1	0
C34M1_027	spt:Q9SSL9	Highly similar to receptor-like protein kinase	236	129	**1634***	242	At1g73080.1	0
6 Cell rescue, defence and virulence, 12 entries (6.5%)								
6.1 Detoxification, 12 entries (6.5%)								
T34M12_036	sp:P20238	Metallothionein-like protein 1	1123	*249**	*699**	*333**	At3g09390.1	4.00E-18
T32M4_014	spt:Q9FNU2	Putative ABC transporter transmembrane protein	1831	**4594***	*801**	*1003**	At5g39040.1	0
T14M1_023	spt:Q9FNU2	Putative ABC transporter transmembrane protein	194	**762***	224	**651***	At5g39040.1	0
T21M12_018	spt:Q9FQE6	Glutathione *S*-transferase GST 12	901	**3734***	840	**3406***	At5g62480.1	2.00E-65
T24M13_029	sp:P25317	Probable glutathione *S*-transferase PARA/auxin-regulated protein PARA	3264	3076	2948	*1658**	At1g17180.1	4.00E-83
T24M13_025	sp:P25317	Probable glutathione *S*-transferase PARA/auxin-regulated protein PARA	167	**1491***	123	**1442***	At1g17180.1	4.00E-83
C13M2_027	spt:Q9FQE6	Glutathione *S*-transferase GST 12	1542	**13 115***	1363	**10 337***	At5g62480.1	2.00E-65
T44M1_020	sp:P25317	Probable glutathione *S*-transferase PARA/auxin-regulated protein PARA	95	**729***	59	**742***	At1g17180.1	4.00E-83
T32M1_022	sp:P25317	Probable glutathione *S*-transferase PARA/auxin-regulated protein PARA	365	**8649***	988	**10 001***	At1g17180.1	4.00E-83
T14M2_036	sp:P25317	Probable glutathione *S*-transferase PARA/auxin-regulated protein PARA	333	**1315***	463	**1246***	At1g17180.1	4.00E-83
T12M1_020	sp:P25317	Probable glutathione *S*-transferase PARA/auxin-regulated protein PARA	684	**2981***	636	**3852***	At1g17180.1	4.00E-83
T14M1_030	sp:P25317	Probable glutathione *S*-transferase PARA/auxin-regulated protein PARA	685	**7592***	1273	**6074***	At1g17180.1	4.00E-83
7 Control of cellular organization, five entries (2.7%)								
7.1 Cell wall, five entries (2.7%)								
T33M2_020	spt:Q9ZP31	Expansin precursor	142	121	**744***	153	At1g26770.1	E-114
C43M3_079	spt:Q8W3 M4	Extensin-like protein	3551	3760	**10 272***	3741	At4g06744.1	0
T31M4_058	spt:O82337	Arabinogalactan protein	718	754	**766***	*242**	At2g46330.1	9.00E-35
T13M3_018	spt:Q6Z387	Lipid transfer protein-like	273	*173**	**875***	207	At2g44300.1	2.00E-35
T21M2_038	sp:P43643	Elongation factor 1-α/vitronectin-like adhesion protein 1 PVN1	660	**2152***	719	1227	At5g60390.1	0
8 Light-related, 11 entries (5.9%)								
8.1 Photosynthesis, six entries (3.2%)								
C43M34_042	spt:Q41003	Chlorophyll *a*/*b* binding protein (fragment)	2311	*2159**	**4126***	2224	At2g34430.1	3.00E-62
T21M24_007	sp:P27492	Chlorophyll *a*/*b* binding protein 16, chloroplast (precursor)	2341	*684**	**5053***	*1468**	At1g29930.1	E-137
T21M44_005	sp:P10707	Chlorophyll *a*/*b* binding protein 1D (fragment)	325	*121**	**1062***	206	At2g34430.1	2.00E-57

Table 1 (Continued)

dTDF	Best hit	Description	Mean band intensity				Arabidopsis closest homologue	
			WT	asCCR	asCAD	DT	AGI	E-value (BLASTP)
T12M2_101	spt:Q84TM7	Chlorophyll *a*/*b* binding protein.	5493	*1543**	**10 817***	*2889**	At2g05100.1	E-138
T13M1_017	spt:O64444	Light-harvesting chlorophyll *a*/*b* –binding protein (precursor)	850	973	*526**	1229	At1g29930.1	E-139
C32M2_023	sp:P13869	Chlorophyll *a*/*b* binding protein, chloroplast (precursor)	350	259	**976***	344	At3g61470.1	E-130
8.2 Photorespiration, one entry (0.5%)								
C24M1_008	spt:Q43775	Glycolate oxidase	1881	*718**	**2699***	**3229***	At3g14420.3	E-147
8.3 Transcriptional control, two entries (1.1%)								
T21M22_033	spt:Q8L5P7	LHY protein	767	1374	**7322***	427	At1g01060.2	E-151
T21M42_046	spt:Q8L5P7	LHY protein	77	63	**394***	41	At1g01060.2	E-151
8.4 Cellular sensing and response, two entries (1.1%)								
T33M3_035	spt:Q9LIE5	Phytochrome A signalling protein	327	379	**5295***	338	At3g22170.1	0
T33M3_034	spt:Q9LIE5	Phytochrome A signalling protein	1710	**5270***	*872**	**2706***	At3g22170.1	0
9. Unclassified proteins, six entries (3.2%)								
T14M3_024	sp:P24422	Probable aquaporin TIP-type RB7-18C	736	*86**	*163**	*66**	At4g17340.1	E-120
T21M3_077	spt:Q93Y38	Transmembrane protein FT27/PFT27-like	6587	*2513**	**9765***	8573	At5g36290.2	E-161
T21M3_072	spt:Q93Y38	Transmembrane protein FT27/PFT27-like	558	**2481***	442	226	At5g36290.2	E-161
T13M2_015	spt:Q9A636	Pentapeptide repeat family protein	291	326	**427***	86	At5g55000.2	8.00E-15
C42M3_056	spt:Q6YAT7	Actin (fragment)	191	**1062***	**2317***	**3217***	At3g12110.1	3.90E-157
C43M34_029	spt:Q6Z8 N9	Putative AT-hook DNA-binding protein	182	**578***	**520***	**686***	At2g33620.3	4.00E-86

For each dTDF, the nearest related gene as obtained by homology search in public databases (see Appendix S1) is given. The identification code and description of the genes was retrieved from the Swiss-Prot database (sp) or from the computer-annotated supplement to Swiss-Prot that contains all the translations of EMBL nucleotide sequence entries not yet integrated in Swiss-Prot, TrEMBL (spt). Transcript levels were scored in the WT and asCCR, asCAD and DT transformants, and the mean band intensity values are given per genotype. One-way ANOVA and *post hoc* LSD tests were carried out. Values significantly different from the WT value at $P < 0.05$ are indicated by asterisks, with italic numbers indicating lower transcript levels, and bold numbers higher transcript levels. The closest Arabidopsis homologue of these genes was searched by sequence comparison at the amino acid level (BLASTP). AGI, Arabidopsis Genome Initiative. dTDFs belonging to the classes of 'expressed protein', 'hypothetical protein', 'unknown protein' and 'no hit' are presented in Table S2.

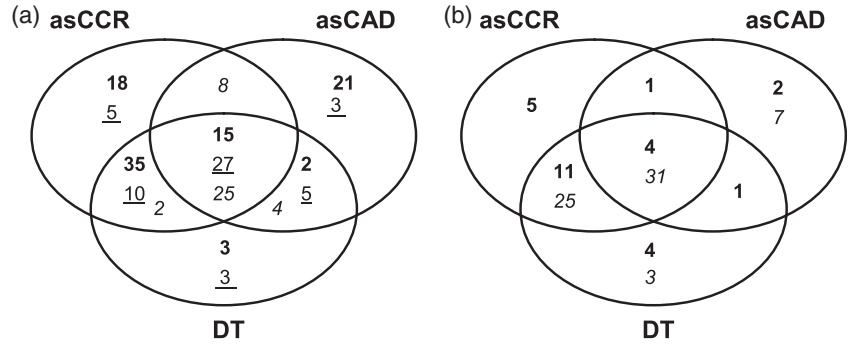

Figure 2. Distribution of dTDFs and metabolites in asCCR, asCAD and DT.
(a) Differential transcripts. Venn diagram indicating the 186 non-redundant dTDFs in the tobacco xylem of asCCR, asCAD or DT based on visual scoring of the cDNA-AFLP gels, ANOVA ($P < 0.05$) and a *post hoc* LSD test of the quantified values and sequencing. Bold, number of dTDFs with higher transcript level as compared to WT; underlined, number of dTDFs with lower transcript level; italics, number of dTDFs that are oppositely regulated in different lines.
(b) Differential metabolites. Venn diagram indicating the number of metabolites that are differential in asCCR, asCAD and DT, as identified by GC-MS (bold) and HPLC (italics). The numbers for GC-MS include only the metabolites with known identity; those for HPLC include metabolites with known and unknown identity.

acid level). Compared to the Arabidopsis *4CL* genes, the dTDF shows equal homology to *At4CL1* and *At4CL2*, which have been proposed as the best candidates for a function in monolignol biosynthesis (Ehlting *et al.*, 1999; Raes *et al.*, 2003), and to the Arabidopsis *4CL*-like genes 5, 6 and 7, for which no role in monolignol biosynthesis has yet been shown. The two *COMT* dTDFs overlap and correspond to a tobacco *COMT* of class I, which is implicated in the biosynthesis of the syringyl units in lignin (Atanassova *et al.*, 1995; Jaeck *et al.*, 1996). The identified *CAD* dTDF is distinct from the *CAD* gene used in the antisense construct to suppress *CAD* expression in asCAD; it is 145 bp long and shares 85% nucleotide identity with the two known tobacco *CAD* cDNAs. The *CAD* dTDF clusters in the class of 'true' *CAD* genes, characterized for their involvement in lignification (Raes *et al.*, 2003).

Also within group 3 are dTDFs corresponding to dihydroflavonol 4-reductase (DFR, a key enzyme in anthocyanin and proanthocyanidin biosynthesis), chorismate mutase (CM, the rate-limiting enzyme in phenylalanine biosynthesis), ADP-glucose pyrophosphorylase (AGPase, the rate-limiting enzyme in starch biosynthesis), glutamate decarboxylase (GAD), and two stress-related transcription factors (a putative heat shock transcription factor and an AP2 domain-containing transcription factor). Finally, dTDFs corresponding to an unknown auxin-responsive gene and an aquaporin were also grouped with the phenylpropanoid biosynthesis genes.

Group 4 (20 dTDFs) consists of genes that were similarly downregulated in asCCR and in DT, and comprised four dTDFs involved in (cell wall) carbohydrate metabolism [UDP-glucose dehydrogenase (UGDH) (two dTDFs), pectin methylesterase (PME) and β-glucosidase]. Additionally, one dTDF of this group corresponded to a sucrose-responsive element binding MYB factor, TSF (Q9FZ15). Other dTDFs of group 4 corresponded to CAB proteins, an adenosine kinase (ADK) and an aminotransferase.

Group 5 (17 dTDFs) represents genes that are mainly strongly upregulated in asCCR but not in DT in which CAD is also deficient. No prevalence of a functional category was apparent. The only dTDF with a known function in metabolism corresponds to glutamine synthetase (GS).

Among the ungrouped dTDFs, all functional categories were represented and some are noteworthy: a dTDF corresponding to an uncharacterized tobacco *PAL* gene was induced in all transformants and most strongly in the *CCR*-deficient lines. When compared to Arabidopsis, this dTDF is most closely related to *AtPAL1* and *AtPAL2* (Raes *et al.*, 2003), hinting at a role for this induced *PAL* gene in lignification. A similar accumulation pattern was seen for the dTDF corresponding to 3-deoxy-D-arabino-heptulosonate-7-phosphate (DAHP) synthase. DAHP synthase regulates the carbon flux into the shikimate pathway (Figure 3). A β-amylase dTDF was induced and an AGPase dTDF was repressed in all transformants, suggesting a general mobilization of starch in CCR- and CAD-deficient plants. Furthermore, dTDFs that might be involved in the transduction of signals from the cell wall to the cytoplasm were mainly found in the CCR-deficient lines. A dTDF corresponding to an arabinogalactan protein (AGP) was strongly repressed specifically in DT. One dTDF corresponded to EF-1α/PVN1, a protein that has been suggested to connect the plasma membrane with the cell wall (Zhu *et al.*, 1994). This dTDF was induced most strongly in the single asCCR transformant. Finally, a dTDF corresponding to a lectin domain-containing RLK was induced specifically in DT.

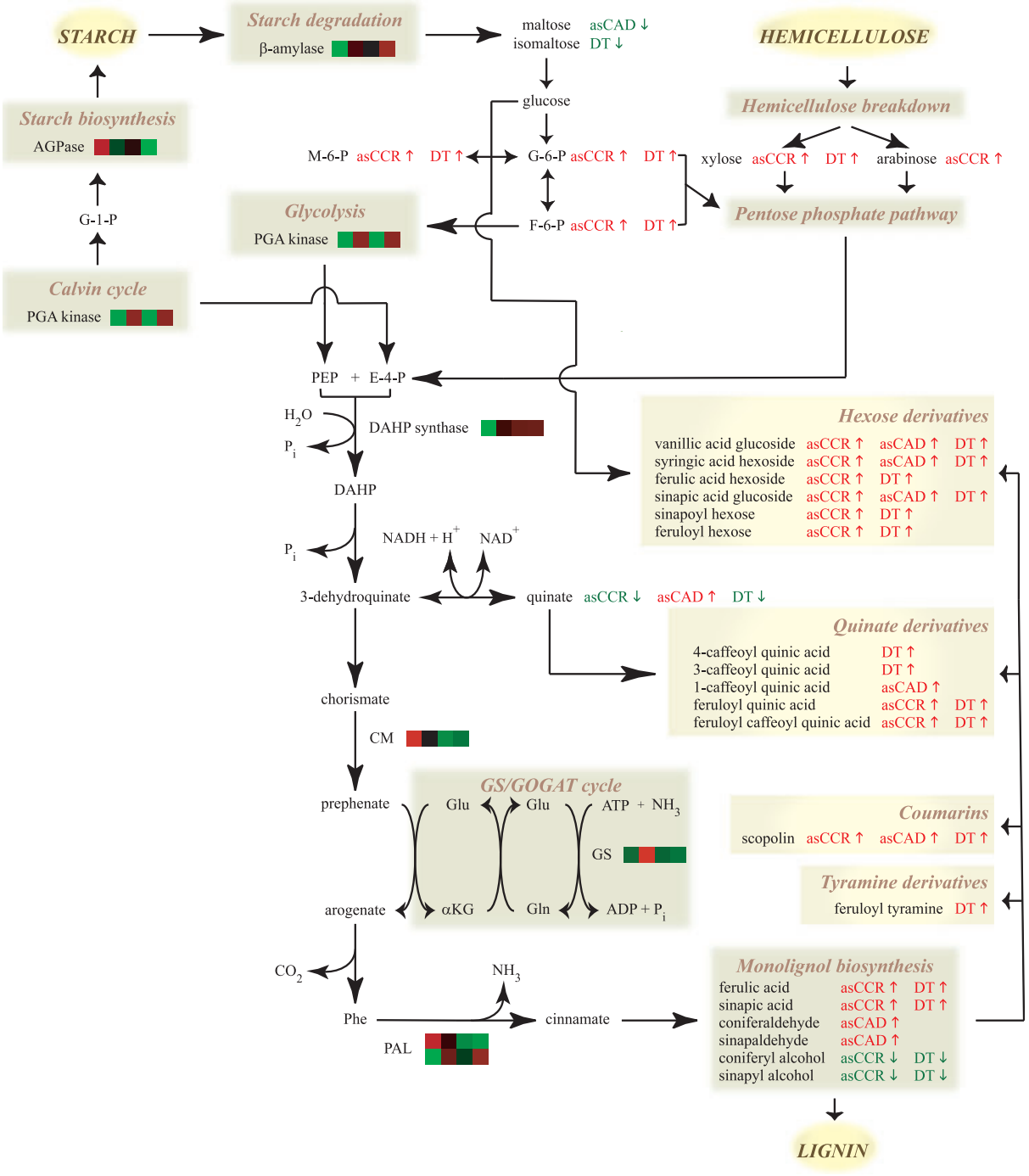

Figure 3. Hypothetical relationship between lignification, respiration and detoxification of accumulating phenylpropanoids.
Several lines of evidence from both the transcript and the metabolite profiles from asCCR, asCAD and DT tobacco reflect an elevated respiration, involving breakdown of starch and elevated glycolytic flux. Increased respiration may be associated with an increased release of glucose and an increased biosynthesis of quinate, which is necessary to store/detoxify the accumulating phenylpropanoid intermediates. The release of glucose from starch breakdown may be destined directly for conjugation with accumulating phenylpropanoids. On the other hand, the induced transcript levels of DAHP synthase in asCCR, asCAD and DT indicate that the elevated carbon flux is extended towards the shikimate pathway, and possibly includes the biosynthesis of quinate. For the genes that displayed differential transcript levels in asCCR, asCAD and/or DT tobacco, transcript profiles of WT, asCCR, asCAD and DT (from left to right) are given. Compounds that display differential accumulation in a given transgenic line are followed by asCCR, asCAD or DT. Red, higher; green, lower. Abbreviations: AGPase, ADP-glucose pyrophosphorylase; G-1-P, glucose-1-phosphate; G-6-P, glucose-6-phosphate; F-6-P, fructose-6-phosphate; M-6-P, mannose-6-phosphate; PGA kinase, 3-phosphoglycerate kinase; E4P, erythrose-4-phosphate; PEP, phospho-*enol*-pyruvate; α-KG, α-ketoglutarate; Gln, glutamine; Glu, glutamate; GS, glutamine synthetase; GOGAT, glutamate synthase; DAHP, 3-deoxy-D-arabino-heptulosonate 7-phosphate; CM, chorismate mutase; PAL, phenylalanine ammonia lyase; asCCR, CCR-downregulated tobacco; asCAD, CAD-downregulated tobacco; DT, tobacco downregulated for both CAD and CCR.

Differential accumulation of phenylpropanoid pathway intermediates and products

Because the altered transcript levels of genes involved in phenylpropanoid metabolism do not necessarily mean that metabolism is altered, it is essential to perform biochemical analyses. Therefore, we first carried out a targeted HPLC-based metabolite profiling of xylem methanol extracts to identify differentially accumulating phenylpropanoid pathway intermediates and products (oligolignols). For this metabolite profiling, a new batch of plants was grown and harvested under the same conditions as for the transcriptome analysis. The set included two lines each for asCAD, asCCR and DT to increase the statistical robustness of the data set. Moreover, all plants were analysed individually (see Experimental procedures). Out of 95 compounds detected, the abundance of 66 compounds was statistically different in at least one of the transgenic lines relative to WT (Table 2; Table S3), of which 18 were below the detection limit in WT and 30 below the detection limit in at least one transgenic line. As was the case for the differential transcriptome, the pattern of differential compounds in DT largely confirmed the pattern in asCCR (Figure 2b), in agreement with the upstream position of CCR relative to CAD in the monolignol biosynthetic pathway. Only three compounds differentially accumulated specifically in DT. The structures of the compounds that were sufficiently pure were resolved by LC–MS analysis (Appendix S1; Figure S2).

Generally, the levels of compounds downstream of CAD and CCR decreased: coniferyl and sinapyl alcohol levels were strongly reduced in asCCR and DT. The levels of 16 oligolignols (oligomers of monolignols and their corresponding aldehydes) were strongly reduced in all transgenic lines, and the abundance of three additional oligolignols was strongly reduced specifically in asCCR and DT. In contrast, the substrates of CAD or CCR, and derivatives thereof, strongly accumulated in the transgenic lines: in asCAD, coniferaldehyde and sinapaldehyde increased, and ferulic acid and sinapic acid increased in asCCR and DT, whereas these four compounds were below the detection limit in WT xylem. In addition, in asCCR and DT, levels of derivatives of ferulic acid and sinapic acid, i.e. ferulic acid hexoside, a feruloyl hexose, feruloyl quinic acid, feruloyl caffeoyl quinic acid, sinapoyl hexose, scopoline, vanillic acid glucoside, sinapic acid glucoside and syringic acid hexoside, were elevated. The latter four compounds also accumulated in asCAD. An increased accumulation of feruloyl tyramine was specifically observed in DT.

Non-targeted metabolite profiling

An unbiased analysis of the metabolite profiles of xylem of WT, asCCR, asCAD and DT was conducted on the same plants as for the targeted phenylpropanoid analysis, by GC-MS profiling and subsequent principal component analysis and univariate statistical tests (Figure S3). Of the compounds with known identity, 28 were differentially present between at least one of the transgenic lines and WT (Table 3; Figure 2b). In addition to GC-MS analysis, the levels of all amino acids were determined with an amino acid analyser (Table 4). Again, most differentially present compounds were found in asCCR and DT. The differential metabolite profiles indicated effects on sugar and hemicellulose metabolism, respiration and photorespiration, as well as the involvement of stress responses. Differentially accumulating metabolites involved in these various metabolic aspects and supporting transcript profiling data are presented in more detail below.

Starch and hemicellulose metabolism and respiration. The differential levels of maltose and isomaltose, which are major products of starch degradation, probably indicate an altered sugar–starch conversion. This observation is in accordance with the general mobilization of starch in CCR- and CAD-deficient plants, as suggested by the lower transcript levels of AGPase and the higher transcript levels of β-amylase; Table 1).

Glucose is used as a substrate for respiration, entering glycolysis via conversion into glucose-6-phosphate (G-6-P) and fructose-6-phosphate (F-6-P). Increased concentrations of the interconvertible G-6-P, F-6-P and mannose-6-phosphate (M-6-P) were detected in asCCR and DT, suggesting elevated respiration (Roessner *et al.*, 2001; Figure 3).

The major hemicellulose present in cell walls of tobacco is arabinoxyloglucan, whose breakdown products are arabinose, xylose and glucose. Increased levels of arabinose in asCCR and xylose in asCCR and DT result from an increased breakdown of hemicellulose compared to WT. The hemicellulose breakdown products, arabinose and xylose can, via conversion to xylulose-5-P, enter the pentose phosphate pathway and function as substrates for respiration (Michal, 1999), or they can be salvaged by converting them back to their UDP conjugates that may re-enter hemicellulose biosynthesis, supporting hemicellulose remodeling (Kotake *et al.*, 2004). Together, these data suggest that the transgenic lines, and mainly asCCR and DT, break down starch and hemicellulose and that the breakdown products enter respiration.

Photorespiration. Citrate levels were increased in all transformants, but no differential accumulation was observed for any other Krebs cycle intermediate. Such specific accumulation of citrate has been associated with elevated photorespiration (Bykova *et al.*, 2005). The levels of the amino acids Gly, Ser, Gln, Glu, Asp and Ala were increased in asCCR and DT (Tables 3 and 4). Elevated levels of the photorespiratory metabolites Gly and Ser, and increased levels of Gln and Glu, have previously been used as indicators for elevated photo-

Table 2 Identified differentially accumulating metabolites in asCCR, asCAD and DT, as revealed by HPLC

t_R	Compound	WT	asCCR	asCAD	DT
5.64	Vanillic acid glucoside	132 ± 10	**602 ± 90**	**485 ± 60**	**985 ± 60**
5.91	Syringic acid hexoside	12.6 ± 2	**357 ± 40**	**52.8 ± 4**	**424 ± 50**
6.59	Ferulic acid hexoside	n.d.	**2420 ± 300**	n.d.	**7670 ± 500**
6.99	Sinapic acid glucoside	n.d.	**4250 ± 500**	**165 ± 30**	**5260 ± 200**
7.13	Scopolin	248 ± 20	**3530 ± 300**	**2700 ± 400**	**5700 ± 300**
7.81	Sinapoyl hexose	n.d.	**72.0 ± 14**	n.d.	**319 ± 30**
7.89	Feruloyl hexose	n.d.	**72.2 ± 10**	n.d.	**166 ± 20**
9.26	Feruloyl quinic acid	n.d.	**343 ± 50**	n.d.	**661 ± 110**
10.08	Sinapyl alcohol	87.5 ± 10	*22.6 ± 5*	115 ± 10	*16.5 ± 3*
10.17	Feruloyl quinic acid	n.d.	**48.6 ± 10**	n.d.	**92.7 ± 11**
10.29	Coniferyl alcohol	36.5 ± 3	*n.d.*	40.0 ± 8	*n.d.*
10.65	**G**(*t*8–O–4)**G**	39.6 ± 2	*n.d.*	110 ± 10	*n.d.*
10.91	**G**(*t*8–O–4)**G**(*t*8–O–4)**G**	67.3 ± 5	*n.d.*	*n.d.*	*n.d.*
11.26	Sinapic acid	n.d.	**32.8 ± 3**	n.d.	**30.3 ± 2**
11.47	Ferulic acid	n.d.	**117 ± 10**	n.d.	**79.0 ± 5**
13.06	Sinapaldehyde	n.d.	n.d.	**52.9 ± 9**	n.d.
13.39	Coniferaldehyde	n.d.	n.d.	**326 ± 40**	n.d.
14.32	Feruloyl caffeoyl quinic acid	n.d.	**53.7 ± 7**	n.d.	**71.2 ± 12**
14.62	**G**(8–5)**G**	544 ± 50	*n.d.*	*27.4 ± 4*	*n.d.*
14.62	**G**(*t*8–O–4)**FT**	–[a]	*n.d.*	n.d.	*n.d.*
15.08	$\mathbf{G^{Me}}$(*t*8–O–4)**G**	42.2 ± 5	*n.d.*	*9.12 ± 1.4*	*n.d.*
15.33	Feruloyl tyramine	36.1 ± 6	38.3 ± 7	45.8 ± 6	**83.3 ± 17**
15.56	**G**(*t*8–O–4)**S**(8–5)**G**	186 ± 20	*n.d.*	*5.96 ± 1.7*	*n.d.*
16.03	**G**(*t*8–O–4)**G**(8–8)**G**	8.64 ± 0.7	*n.d.*	*n.d.*	*n.d.*
16.22	**G**(*t*8–O–4)**G**(8–5)**G′**	14.9 ± 1	*n.d.*	*n.d.*	*n.d.*
16.38	**G**(*e*8–O–4)**G**(8–5)**G′**	66.3 ± 6	*n.d.*	*4.09 ± 0.7*	*n.d.*
16.66	**G**(8–8)**G**	12.5 ± 6	*n.d.*	1.03 ± 0.2	*n.d.*
17.10	**G**(8–O–4)**G**(8–8)**S**(8–O–4)**G**	40.2 ± 5	*n.d.*	*11.5 ± 1*	*n.d.*
17.28	**G**(8–5)**G′**	93.2 ± 12	*n.d.*	*29.3 ± 4*	*n.d.*
17.48	***G**(*t*8–O–4)**S**(8–8)**G**	49.5 ± 5	*n.d.*	*8.11 ± 1.2*	*n.d.*
17.75	**G**(*t*8–O–4)**S**(8–5)**G′**	30.9 ± 4	*n.d.*	*9.29 ± 1.8*	*n.d.*
17.94	***G**(*t*8–O–4)**S**(8–8)**G**	25.4 ± 2	*12.5 ± 3*	*1.65 ± 0.4*	*18.3 ± 3*
18.41	**G**(*t*8–O–4)**S**(8–8)**S**	36.7 ± 3	*n.d.*	*3.25 ± 0.7*	*n.d.*
18.64	**G**(*e*8–O–4)**S**(8–8)**G**	18.0 ± 3	*n.d.*	*3.86 ± 0.8*	*n.d.*
18.98	$\mathbf{G^{Me}}$(*t*8–O–4)**S**(8–5)**G**	23.6 ± 3	*n.d.*	18.2 ± 2	*n.d.*
19.16	**G**(8–O–4)**S**(8–8)**S**(8–O–4)**G**	21.8 ± 3	*n.d.*	*2.60 ± 0.8*	*n.d.*

Values are expressed as μV mg^{-1} dry weight; values significantly different from WT at $P < 0.05$ are indicated in bold or italics, respectively, when they are higher or lower in abundance. *n.d.*, not detected.

[a]Compound detected by MS, but co-elution hampered its quantification by UV/Vis; asterisks indicate compounds that are stereoisomers. Caffeoyl quinates were detected, but could not be quantified because of co-elution. Nomenclature is as described by Morreel *et al.* (2004a). Transgenic lines and number of plants analysed are described in Experimental procedures. Values are means ± SE. Only the differentially accumulating metabolites with known identities are shown; those with unknown identities are presented in Table S3.

respiration (Jeong *et al.*, 2004; Kozaki and Takeba, 1996; Oliveira *et al.*, 2002). Gln and Glu are intermediates in the re-assimilation of photorespiratory ammonium via the glutamine synthetase/glutamate synthase (GS/GOGAT) cycle. Asp and Ala are derived from Glu. Together with the dTDFs corresponding to the photorespiratory enzymes glycolate oxidase and GS, these differential metabolites indicate altered photorespiration in asCCR and DT.

Indicators of a stress response. Other metabolic changes, such as the altered levels of trehalose, raffinose and galactinol, the phenolic compound caffeoyl quinic acid, and the metabolites involved in polyamine biosynthesis, i.e. Arg, putrescine, β-alanine and γ-amino butyric acid (GABA), point towards a potential stress response in the transgenic plants, mostly in asCCR and DT [trehalose (Wingler, 2002); raffinose and galactinol (Panikulangara *et al.*, 2004); polyamines (Kaplan *et al.*, 2004; Nikiforova *et al.*, 2005)].

Taken together with the transcriptome data that indicate altered transcript levels for metallothioneins, GSTs and heat shock transcription factors, which are typical defence genes induced in response to oxidative damage, the differential accumulation of stress-related metabolites revealed by GC-MS indicates that CCR deficiency may result in oxidative stress in tobacco.

Table 3 Differentially accumulating metabolites in asCCR, asCAD and DT, as identified by GC-MS

		PCA			asCCR		asCAD		DT	
Compound	ID	PC1	PC3	PC4	*P*-value	Fold change	*P*-value	Fold change	*P*-value	Fold change
Sugar metabolism										
Trehalose	274 002	0.87	−0.25				<0.05	**2.2**		
Raffinose	337 002	0.9	−0.26				<0.01	**2.8**	<0.05	*0.7*
Melezitose	346 001	0.88			<0.05	**1.6**	<0.01	**2.6**		
Galactinol	299 002		0.53		<0.001	**1.8**				
myo-Inositol	209 002		−0.59						<0.001	*0.6*
Isomaltose	287 001	0.8	−0.45						<0.001	*0.3*
Maltose	274 001	0.91					0.06	*0.6*		
Respiration										
Fructose-6-phosphate	232 002		0.56		<0.01	**1.9**			<0.0001	**2.1**
Glucose-6-phosphate	235 002		0.64		<0.0001	**2.5**			<0.0001	**2.6**
Mannose-6-phosphate	231 001		0.58		<0.01	**1.8**			<0.0001	**1.9**
Galactose-6-phosphate	232 001		0.56		<0.01	**1.7**			<0.001	**2**
Citric acid	182 004	0.85			<0.001	**2.1**	<0.01	**3.1**	<0.05	**1.3**
Hemicellulose metabolism										
Xylose	166 001		0.47	0.28	<0.0001	**2.4**			<0.001	**1.9**
Arabinose	167 002		−0.22	0.34	<0.05	**1.3**				
Amino acids and polyamines										
Putrescine	175 002	0.84			<0.01	**2.1**	<0.05	**2.2**	<0.05	**1.6**
γ-Amino butyric acid	153 003		0.45	0.31	<0.0001	**2.3**			<0.05	**1.7**
β-Alanine	144 001		0.41		<0.05	**1.5**				
Serine	138 001		0.40	0.26	<0.01	**1.8**				
Threonine	140 001		0.54	0.41	<0.01	**1.9**				
Glutamic acid	163 001		0.55	0.52	<0.0001	**2.7**			<0.001	**1.8**
Tyrosine	194 002		0.64	−0.24	<0.001	**3.7**			<0.0001	**6**
Methionine	152 001			0.3	<0.0001	**1.9**			<0.01	**1.5**
Other										
D-Quinic acid	185 001	0.72	−0.56		<0.001	*0.5*	<0.05	**1.9**	<0.0001	*0.4*
4-Caffeoyl quinic acid	317 001	−0.29	0.39						<0.001	**2.5**
3-Caffeoyl quinic acid	311 001								<0.0001	**3.6**
1-Caffeoyl quinic acid	340 001	0.84	−0.28				<0.05	**2.1**		
Pyroglutamic acid	153 002		0.40	0.53	<0.0001	**2.3**			<0.001	**1.6**
Threonic acid	156 001		−0.34	0.28	<0.05	*0.5*			<0.01	*0.4*
Glycerol	129 003		−0.5		<0.001	*0.5*	<0.01	**2.7**	<0.0001	*0.5*

ID, mass spectral identifier (see Experimental procedures); PCA, principal component analysis; PC, principal component; *P*, significance. PC1 separated asCAD from the other tobacco lines, whereas asCCR and DT were distinguished from the other tobacco lines by PC3. PC4 was involved in the distinction between asCCR and DT. The loading factors of those compounds that contributed prominently (see Experimental procedures) to PC1, PC3 and/or PC4 are shown. Italics, lower abundance; bold, higher abundance compared with WT. Transgenic lines and the number of plants analysed are described in Experimental procedures.

Photo-oxidative stress. The altered threonic acid and pyroglutamic acid concentrations in asCCR and DT may indicate altered redox status in the chloroplast, reflecting photo-oxidative stress. Threonic acid and pyroglutamic acid are derived from L-ascorbate and glutathione (GSH), respectively, which constitute, via the 'ascorbate–glutathione cycle', two major anti-oxidants of the chloroplast's photo-oxidative stress defence system (Bray *et al.*, 2000). Photo-oxidative stress was also suggested by the transcriptome data. One dTDF was most homologous to a thylakoid-located FtsH protease that is probably involved in the degradation of photo-oxidatively damaged photosystem II (PSII) proteins (Lindahl *et al.*, 1996), and three dTDFs corresponded with chloroplastic ribosomal proteins. Furthermore, one dTDF corresponded to an epoxide hydrolase that is possibly functional in the xanthophyll cycle involved in photoprotective energy dissipation (Loggini *et al.*, 1999). Taken together, both transcriptome and metabolome data indicate photo-oxidative stress in the lignin-modified lines, again predominantly in asCCR and DT.

Validation of hypotheses generated by molecular phenotyping

Pigments. Various methods were used to validate the hypotheses generated on the basis of the molecular phenotyping. Transcript profiling data suggested there were effects on pigment biosynthesis in the transformants. A

Table 4 Amino acid concentration in WT, asCCR, asCAD and DT, as determined by HPLC

	Peak height (μAU μg^{-1} dry weight; mean ± SE)			
Amino acid	WT	asCCR	asCAD	DT
Asp*	107 ± 10	**268 ± 30**	133 ± 10	**239 ± 20**
Glu	218 ± 20	506 ± 60	216 ± 20	451 ± 30
Asn	14.0 ± 2	35.3 ± 4	17.3 ± 1	31.1 ± 2
Ser*	21.8 ± 3	**39.6 ± 4**	25.9 ± 5	**34.0 ± 3**
Gln*	107 ± 10	**179 ± 20**	90.3 ± 6	**143 ± 11**
Gly*	8.49 ± 1.1	**12.2 ± 1**	8.07 ± 1.1	**12.2 ± 1**
His*	4.61 ± 0.4	6.21 ± 0.8	5.45 ± 0.6	**8.37 ± 1.1**
Arg*	4.72 ± 0.3	**6.89 ± 0.8**	5.08 ± 0.3	**6.69 ± 0.6**
Thr	31.8 ± 4	57.9 ± 5	29.0 ± 3	49.3 ± 3
Ala*	23.1 ± 3	**77.3 ± 10**	49.7 ± 7	**98.4 ± 7**
Pro	10.7 ± 1	42.0 ± 8	9.13 ± 1.1	16.2 ± 1
Tyr*	10.4 ± 1	**22.9 ± 2**	11.1 ± 1	**24.2 ± 1**
Val	14.6 ± 2	23.3 ± 1	16.2 ± 2	51.6 ± 32
Met	4.18 ± 0.4	4.72 ± 0.6	22.3 ± 5	5.99 ± 0.8
Cystine*	n.d.	0.551 ± 0.55	**16.1 ± 4**	n.d.
Ile	7.08 ± 1.0	9.71 ± 0.8	6.67 ± 1.2	11.0 ± 1
Leu	26.6 ± 2	41.7 ± 3	21.8 ± 2	38.6 ± 1
Phe	11.8 ± 1	11.7 ± 1	9.76 ± 1.0	12.1 ± 1
Trp	7.05 ± 1.1	8.00 ± 0.7	5.64 ± 0.9	8.96 ± 0.9
Lys	10.0 ± 1	8.67 ± 0.6	5.75 ± 0.8	9.15 ± 0.6

*Amino acids of either asCCR, asCAD or DT that accumulate differentially in both transgenic lines compared with WT at $P < 0.05$. Bold, higher abundance compared to WT. n.d., not detected. Transgenic lines and the number of plants analysed are described in Experimental procedures.

Table 5 Pigment concentrations

Pigment	WT	asCCR	asCAD	DT
Xylem				
ChlA	74.7 ± 4	**146 ± 10**	**135 ± 10**	**171 ± 10**
ChlB	25.1 ± 3	41.5 ± 3	53.0 ± 6	55.6 ± 6
Carotenoid	36.0 ± 3	**77.4 ± 3**	**77.3 ± 3**	**84.6 ± 5**
Anthocyanin	1.73 ± 0.3	1.32 ± 0.3	*0.872 ± 0.16*	*0.727 ± 0.21*
Cortex				
ChlA	527 ± 20	**1540 ± 100**	**995 ± 60**	**1450 ± 100**
ChlB	177 ± 10	**449 ± 30**	290 ± 20	**498 ± 80**
Carotenoid	175 ± 10	**445 ± 30**	**317 ± 20**	**399 ± 40**
Anthocyanin	0.197 ± 0.29	−3.10 ± 0.4	0.442 ± 0.68	−3.42 ± 0.6
Leaf				
ChlA	563 ± 40	**952 ± 60**	**1730 ± 700**	**1330 ± 100**
ChlB	170 ± 10	236 ± 20	423 ± 180	**348 ± 30**
Carotenoid	164 ± 10	249 ± 20	**463 ± 200**	**352 ± 30**
Anthocyanin	−0.896 ± 0.21	*−3.95 ± 0.3*	*−3.56 ± 0.4*	*−4.04 ± 0.2*

Chlorophyll *a* and *b* and carotenoid data are mean concentrations (±SE) in $\mu g\ mg^{-1}$ dry weight, anthocyanin data are absorbance values (±SE). Values significantly different from WT at $P < 0.05$ have a different font: bold, increased concentration; italics, decreased concentration. Transgenic lines and the number of plants analysed are described in Experimental procedures.

general repression of chloroplast-localized steroid biosynthesis was prompted by the reduced transcript levels, particularly in DT, of 1-deoxy-D-xylulose-5-phosphate synthase, a key enzyme in the biosynthesis of chloroplast-bound isoprenoids, such as carotenoids (carotenes and xanthophylls), prenyl chains of chlorophylls and plastoquinone-9 (important in plant respiration), and ABA. On the other hand, reduced *DFR* transcript levels (in asCCR, asCAD and DT) suggested reduced levels of anthocyanins.

To check for altered pigment accumulation, chlorophyll *a* (ChlA), chlorophyll *b* (ChlB), carotenoids and anthocyanins were quantified spectrophotometrically in extracts from xylem, cortex and leaves (Table 5). ChlA levels (and to a lesser extent ChlB levels) were markedly increased in leaf, xylem and cortex of all transgenic lines. Anthocyanin levels were significantly reduced in leaves of all transgenic lines, whereas, in xylem, a significant decrease in anthocyanin and carotenoid content was only obvious in asCAD and DT.

Chlorophyll fluorescence and efficiency of photochemistry. The differential transcriptome and metabolome, together with the elevated chlorophyll content, suggested over-excitation of the photosynthetic apparatus, photo-oxidative damage, and alterations at the levels of photosynthesis and photorespiration in the transformants. To test whether the profiling data truly reflected changes in these physiological processes *in planta*, chlorophyll fluorescence and gas exchange were measured.

Fluorescence from leaves of WT, asCCR, asCAD and DT in the dark-acclimatized state upon application of a saturating flash gives an indication of the maximal amount of absorbed light that can be used to drive the electron transport chain, allowing determination of the maximum photochemical quantum yield of PSII (F_v/F_m) in the absence of non-photochemical quenching. The F_v/F_m ratio in the yellowish tissue between the leaf veins of asCCR and DT was significantly decreased when compared to WT (Table 6). In contrast, when measurements were performed on the dark-green tissue surrounding the lesions, a significant increase in F_v/F_m was observed in asCCR and DT. Chlorophyll fluorescence parameters measured in the light-acclimatized state give an indication of the actual proportion of photochemical and non-photochemical quenching. The actual proportion of absorbed light that is used to drive the electron transport chain is represented by the photochemical quantum yield Φ_{PSII}, and was significantly increased in asCCR and DT. In the other lines that were tested, no significant changes in fluorescence parameters were apparent.

Gas exchange. The increase in the photochemical quantum yield of PSII may result in altered photosynthesis and/or photorespiration. Because photorespiration measurements are time-consuming, and, for optimal comparability,

Table 6 Fluorescence

	WT	asCCR	DT	$P_{enz/tr}$	P_{tr}	P_{model}
F_v/F_m	0.779 ± 0.01	0.796 ± 0.01*	0.790 ± 0.01			0.0467
F_v/F_m (lesions)		0.758 ± 0.01*	0.747 ± 0.01*			
Φ_{PSII}	0.132 ± 0.01	0.183 ± 0.02*	0.156 ± 0.01*	0.313	0.017	0.0532

Chlorophyll fluorescence variables of the youngest mature leaf of tobacco plants. Measurements were obtained in the dark-acclimatized (F_v/F_m) and light-acclimatized states (Φ_{PSII}). Means ± SE are indicated. F_v/F_m measurements for asCCR and DT were made on leaf sections avoiding and focusing on the lesions. Asterisks indicate values that are significantly different from the WT ($P < 0.10$). F_v/F_m, maximum photochemical quantum yield of PSII; Φ_{PSII}, photochemical quantum yield of PSII. Transgenic lines and the number of plants analysed are described in Experimental procedures.

should be performed in the shortest possible time interval, we first assayed a limited set of asCAD, asCCR and DT lines. Differential photorespiration was most obvious in the homozygous CCR-deficient transformants asCCR (B3.1) and DT (Dt52.6) (data not shown). These lines were further examined by gas exchange tests (Table 7). Photorespiration was significantly increased in both asCCR (B3.1) and DT (Dt52.6), whereas no significant effects on photosynthesis were observed.

Discussion

Characterization of the molecular phenotype by transcriptome and metabolome profiling

In an attempt to map the metabolic sphere of influence of the perturbation of an essentially structural process, lignification, alterations in transcript and metabolite levels were studied in the xylem of tobacco plants in which the expression of CCR, CAD or both were downregulated. We hypothesized that interpretation of the snapshots of the differential transcriptomes and metabolomes of the transformants would help reveal the molecular and metabolic processes that are associated with the morphological phenotypes that have been described for these transformants by Chabannes *et al.* (2001a). Supporting this presumption, the molecular phenotypes were proportional to the morphological phenotypes (Chabannes *et al.*, 2001a; Halpin *et al.*, 1994; Piquemal *et al.*, 1998); a more restricted portion of the transcriptome was affected in asCAD than in asCCR, and this tendency was also evident at the metabolite level. Furthermore, when both CCR and CAD were deficient (in the DT), the effects of downregulation of the most upstream enzyme, CCR, prevailed both at the transcriptome and metabolome levels. Phenylpropanoid biosynthesis was affected in asCAD as well as in asCCR and DT. However, a clear distinction was apparent between CCR and CAD downregulated plants with regard to the functions of the other affected metabolic pathways. The molecular phenotype of asCCR and DT was characterized mainly by changes at the level of detoxification and carbohydrate metabolism, whereas the molecular phenotype of asCAD was enriched by differential transcript levels of light- and cell-wall-related genes. Interpretation of the differences at the level of the transcriptome and metabolome, although obtained from distinct plant batches because of practical restrictions, led to a coherent image of the molecular adaptations in these transgenic plants.

Table 7 Gas exchange analyses

Tobacco line	A_{sat} (μmol m^{-2} sec^{-1})	Photorespiration (μmol m^{-2} sec^{-1})
WT	14.01 ± 0.6	6.57 ± 0.2
B3.1	14.62 ± 0.6	7.87 ± 0.3*
Dt52.6	12.85 ± 0.7	7.61 ± 0.2*
P_{model}	0.1422	0.0020

CO_2 assimilation rate at saturating light intensity (A_{sat}) in air containing 21% O_2 and rates of photorespiration of the youngest mature leaf of WT, asCCR and DT. Means ± SE are given. Asterisks indicate values that are significantly different ($P < 0.10$) from WT. Transgenic lines and the number of plants analysed are described in Experimental procedures.

Candidate genes for a function in the control of lignin biosynthesis-associated processes

Transcript profiling revealed differential expression in the three transgenic lines (asCCR, asCAD and DT) of genes involved in monolignol biosynthesis (*CAD* and *COMT*), in the general phenylpropanoid pathway (*PAL*, *4CL*) and in the substrate-supplying shikimate-aromatic amino acid biosynthesis pathway (*CM*). With the exception of one of the two differential *PAL* genes, all these monolignol biosynthesis-linked genes were similarly downregulated in asCCR, asCAD and DT. These data prove that our approach is valid to identify genes that are metabolically closely linked to phenylpropanoid metabolism. Hence, the set of known and unknown genes whose transcript levels were similarly downregulated in asCCR, asCAD and DT (Figure S1) are good additional candidates to be closely associated with the pathway.

Comparison of the transcript profiling data with those obtained for other mutants in the monolignol biosynthetic pathway also pointed to a set of interesting candidate genes that are likely to play a role in flux control through primary and secondary metabolism in response to changes in monolignol biosynthesis. For example, for many genes that displayed altered transcript levels in asCCR, asCAD or DT, i.e. those encoding PAL, 4CL, COMT, CM, PGA Kinase, β-glucosidase, glycolate oxidase, AGPase, DAHP, UGDH, GAD, β-amylase and GS, the closest Arabidopsis homo-

logues were also differentially expressed in Arabidopsis *cad-c cad-d*, *pal1*, *pal2* and/or *c3h* mutants (Abdulrazzak *et al.*, 2006; Rohde *et al.*, 2004; Sibout *et al.*, 2005). Therefore, the corresponding enzymes are good candidates for a direct or indirect flux-controlling role in lignin-associated processes.

Two transcription factor genes displayed a similarly strong downregulated transcript level in asCAD and asCCR lines, as was observed for the phenylpropanoid biosynthesis genes. These genes, encoding a putative heat shock transcription factor and an AP2 domain-containing transcription factor, might have a putative function in the coordinated transcriptional regulation of phenylpropanoid metabolism. This hypothesis is further supported by the fact that the transcript level of the closest Arabidopsis homologue of the AP2 transcription factor (At3g16770) was reduced in the Arabidopsis *cad-c cad-d* mutant (Sibout *et al.*, 2005). In contrast, the Myb-like transcription factor DIVARICATA was induced in the asCCR and DT lines, and may be induced in response to low lignin contents. Its closest Arabidopsis homologue (At5g5890) is similarly induced in an Arabidopsis *c3h* insertion mutant (Abdulrazzak *et al.*, 2006).

Based on their differential transcript levels in various transgenic lines/mutants with defects in monolignol biosynthesis, several signal transduction genes are good candidates for a regulatory function associated with lignification: an *RLK* showing differential transcript levels in asCAD tobacco and whose closest Arabidopsis homologue (At1g73080) is differentially expressed in the *cad-c cad-d* and *pal1* Arabidopsis mutants (Rohde *et al.*, 2004; Sibout *et al.*, 2005), a gene encoding a PHYA signalling protein that has differential transcript levels in asCCR, asCAD and DT and whose closest Arabidopsis homologue (At3g22170) is differentially expressed in the *pal2* Arabidopsis mutant (Rohde *et al.*, 2004), and a phosphatidylinositol-4-phosphate 5-kinase with differential transcript levels in asCAD tobacco and whose closest Arabidopsis homologue (At1g21920) is differentially expressed in the *pal1* and *pal1 pal2* mutants (Rohde *et al.*, 2004).

Because auxin is a key signal for secondary xylem formation (Sundberg *et al.*, 2000), an unknown auxin-responsive gene, which was identified here, with reduced transcript levels in asCCR, asCAD and DT, and six tags corresponding to the auxin-related GST parA, upregulated in asCCR and DT, might play a role in integration of monolignol biosynthesis into the developmental process of secondary xylem formation. Additionally, an aquaporin with a highly similar transcript profile as this auxin-responsive protein across the transgenic tobacco lines might be involved in the coordinated cyclic regulation of cell expansion and lignification during secondary xylem formation (Harmer *et al.*, 2000). Aquaporins mediate the water influx associated with cell expansion. Because expression of the closest Arabidopsis homologue of both the auxin-responsive unknown (At3g25290) and aquaporin (At4g17340) genes were reduced as well in the *cad-c cad-d* mutant (Sibout *et al.*, 2005) we believe that these genes are worthy targets for further functional studies.

Lignin biosynthesis and starch metabolism are closely linked

In xylem cells, a major portion of the carbon that is channelled into phenylpropanoid metabolism is diverted to lignin biosynthesis (van Heerden *et al.*, 1996). The flux into secondary metabolism can be limited by the precursor supply in primary metabolism (Henkes *et al.*, 2001; Rogers *et al.*, 2005). In plants, starch is the major carbon storage form and sucrose the major carbon transport form, and the latter may be considered as the main substrate for lignin biosynthesis (Amthor, 2003). A dependency of the transcript levels of lignin biosynthetic genes on starch turnover and availability of sucrose has been demonstrated in the Arabidopsis *sex1* mutant. This mutant is impaired in its ability to degrade starch granules, has low transcript levels of most monolignol biosynthetic genes, and accumulates less lignin (Rogers *et al.*, 2005). In the transgenic tobacco lines analysed, the opposite effect was apparent; in concert with a general downregulation of phenylpropanoid biosynthesis genes in asCCR, asCAD and DT, the transcript levels of a rate-determining starch biosynthetic enzyme, AGPase, were reduced, and those of a starch-degrading exo-enzyme, β-amylase, were induced. These observations indicate a general induction of starch mobilization that is linked with monolignol biosynthesis. Alterations in starch and sucrose metabolism were further supported by the altered levels of maltose and isomaltose.

Metabolic link between the detoxification of accumulating phenylpropanoid intermediates and carbon supply

In asCAD, the substrates of the suppressed enzyme, coniferaldehyde and sinapaldehyde, accumulated strongly, whereas in asCCR and DT, the abundances of glycosylated and quinylated derivatives of the substrate of CCR, feruloyl CoA, and, additionally, ferulic acid and sinapic acid were strongly elevated. Similar to what was proposed for CCoAOMT-deficient plants, feruloyl CoA, the substrate of CCR, might be quinylated or re-directed to ferulate by a thioesterase. Ferulic acid would then be partially converted to sinapic acid, and both acids detoxified by glycosylation (Guo *et al.*, 2001; Meyermans *et al.*, 2000).

The accumulation of glycosylated and quinylated phenylpropanoid derivatives, which is particularly strong in asCCR and DT, indicates that the accumulation of monolignol biosynthesis intermediates in CCR- and/or CAD-deficient plants provokes a concomitant induction of the detoxifica-

tion and storage mechanisms, requiring, in turn, an increased carbon supply in the form of glucose and quinate. Where do the glucose and quinate come from? In asCAD, asCCR and DT, the lower transcript levels for AGPase and the higher transcript levels for β-amylase than in WT indicated a reduced biosynthesis and increased degradation of starch to glucose. In asCCR and DT, several lines of evidence from both the transcript and the metabolite profiles additionally reflected an elevated respiration, involving the breakdown of carbohydrate polymers or oligomers to glucose, followed by the utilization of glucose by the glycolytic pathway. The release of glucose from starch or hemicellulose catabolism may be destined directly for conjugation with accumulating phenylpropanoids. On the other hand, the induced transcript levels of DAHP synthase in asCCR, asCAD and DT indicate that the elevated carbon flux is at least partly extended towards the shikimate pathway, and, because *CM* transcript levels are reduced in these lines, an increased flux towards the biosynthesis of quinate is expected. The level of free quinate then depends on the balance between quinate biosynthesis and quinate acylation. Free quinate levels are increased in the asCAD plants but are decreased in the asCCR and DT plants. A stronger depletion of quinate in the asCCR plants is in accordance with the stronger accumulation of phenylpropanoid quinic esters in these plants, and does not contradict a concomitant increase of quinate biosynthesis (Figure 3).

A link between cell-wall expansion and light-related genes is apparent in asCAD

Specifically, in asCAD tobacco, the transcript levels of several genes related to cell-wall expansion (expansin, LTP, PGase, PME), and of genes involved in the light-harvesting complex/circadian clock (*CAB, LHY*, and PHYA), and light signalling (*PhyA*), were elevated. Similarly, microarray analyses of the xylem of transgenic CAD-downregulated poplar (*Populus tremula* x *alba*) revealed differential transcript levels of predominantly light/circadian clock-related genes, including *CAB* and *LHY* (Andersson Gunneråas, 2005), and an important fraction of differentially expressed genes in Arabidopsis *cad* mutants encoded cell-wall (expansion) proteins (Sibout *et al.*, 2005). These data suggest unanticipated alterations of cell-wall structure in asCAD that have so far remained unnoticed. Further detailed experiments are required to reveal these effects at the structural level.

Oxidative stress

Differential transcript levels of stress-related genes and the accumulation of low-molecular-weight anti-oxidants and other stress-related compounds, particularly in the CCR-deficient plants, indicate that the transgenic plants experience oxidative stress. What could trigger oxidative stress in plants with perturbed monolignol biosynthesis? One reason could be that the anti-oxidant defence system is partly deficient. In some plant species, hydroxycinnamic acids play an important role as anti-oxidants (Neill *et al.*, 2002). In tobacco plants with inhibited phenylpropanoid metabolism caused by overexpression of the transcription factor AmMYB308, or with inhibited *PAL* expression, premature cell death in the leaves has been reported, a phenotype similar to that in the leaves of CCR-deficient tobacco (Elkind *et al.*, 1990; Tamagnone *et al.*, 1998a), and the decreased levels of phenolic acid derivatives, and particularly caffeoyl quinic acid, have been suggested to be the cause of the oxidative stress (Tamagnone *et al.*, 1998b). However, in CCR- and CAD-deficient tobacco, the levels of hydroxycinnamic acids and their derivatives, including caffeoyl quinic acid, were increased, making this hypothesis not very likely.

On the other hand, anthocyanins are excellent scavengers of free radicals. High light induces anthocyanin accumulation that might protect plants against photo-oxidative stress and cell death (Vandenabeele *et al.*, 2004; Vanderauwera *et al.*, 2005). The decreased anthocyanin levels in the xylem of asCAD and DT and in the leaves of asCCR, asCAD and DT might thus contribute to oxidative stress. Anthocyanin levels were indeed most severely decreased in the lines that developed lesions in the leaves. However, the possibility cannot be excluded that the observed decrease in anthocyanin levels are a secondary effect of oxidative stress rather than its cause. Indeed, transcriptome analysis of catalase-deficient Arabidopsis indicated that accumulating H_2O_2 impairs the high-light induction of genes involved in the regulation, biosynthesis and sequestration of anthocyanins (Vandenabeele *et al.*, 2004; Vanderauwera *et al.*, 2005).

The altered cell wall as a stress generator

Alternatively, the molecular stress phenotype may not be primarily due to a defective anti-oxidant defense system, but may be actively induced. One possibility is that the altered cell wall mimics wounding or the early stages of pathogenesis when hydrolysing enzymes secreted by pathogens depolymerize the plant cell wall. An induction of the physiological response characteristic of wounded and infected plants has been described previously for the cellulose synthase mutant *cev1*, whose altered cell wall has been proposed to allow increased release of elicitors (Ellis *et al.*, 2002). In agreement with a wound response, feruloyl tyramine levels were higher in CCR-downregulated lines, both as a soluble compound (this study) and incorporated into the wall (Chabannes *et al.*, 2001a; Ralph *et al.*, 1998). Feruloyl tyramine is an amide formed by the conjugation of tyramine with feruloyl CoA, and is typically elicited in solanaceous plants upon wounding or pathogen attack to rein-

force the cell wall by cross-linking with lignin (Guillet and De Luca, 2005).

A second possibility is that the altered structure of the cell wall itself may signal a stress response. Lignin content is strongly reduced in asCCR and DT, and structural disorders are clearly visible in the xylem cell walls (Chabannes *et al.*, 2001b). Furthermore, alterations in the metabolism of hemicellulose and pectin were apparent from the differential transcriptome and metabolome of the CCR-deficient transformants. Similar alterations in cell-wall biogenesis were observed in cellulose synthase mutants and in the lignin-deficient Arabidopsis *c3h* mutant (Abdulrazzak *et al.*, 2006; Caño-Delgado *et al.*, 2003). Because hemicellulose cross-links the cellulose microfibrils, reduced hemicellulose content might, in turn, contribute to the loss of cohesion of the cell walls observed in asCCR and DT. Ultimately, alterations in cell-wall structure need to be signalled to the nucleus to regulate gene expression. Integrin-like linkages between the cell wall and the plasma membrane are required to mediate some of the signals that can activate defence responses (Mellersh and Heath, 2001). The differentially expressed genes encoding potential linking proteins in the CCR-deficient transformants (AGP, RLKs and EF-1α/PVN1) are thus candidate signal transducers.

Photorespiration dissipates increased photosynthetic efficiency

Another possibility is that the oxidative stress is caused by photorespiratory H_2O_2. An increase in photorespiration was suggested by the differential transcript and metabolite profiles, and was confirmed in asCCR and DT by gas-exchange experiments. Photorespiration is a photoprotective mechanism that dissipates excess electron flow through the photosynthetic apparatus when excess light is absorbed, and is an important source of H_2O_2. In accordance with an induction of photorespiration in response to excess light absorption in the CCR-deficient plants, an increased turnover of PSII proteins was apparent from the transcript profiling, and strong accumulation of H_2O_2 could be visualized in the leaves of the CCR-deficient lines (Figure S4). Moreover, the strongly CCR-downregulated lines had lesions in the leaves that were highly similar to those in catalase-deficient tobacco when grown under high light conditions (Dat *et al.*, 2003), and may thus result from the photo-oxidative stress and subsequent photo-inhibition.

The elevated photorespiration itself is probably caused by the increased efficiency of PSII. Indeed, the electron flow in the photosynthetic electron transport chain depends on the efficiency of the absorption of light energy and the efficiency of the photosynthetic assimilation of CO_2. An increased efficiency of PSII was suggested by increased chlorophyll levels in leaves, cortex and xylem of CCR- and CAD-downregulated transformants. Chlorophyll fluorescence parameters confirmed an increased maximum photochemical quantum yield and an increased PSII efficiency in the leaves of the strongly CCR-downregulated transformants. However, gas-exchange analyses showed that photosynthetic CO_2 assimilation was not significantly altered in these lines. The absorption of more light energy than can be utilized for photosynthesis may increase the level of photorespiration to protect the photosynthetic apparatus from light-induced damage (Niyogi, 2000). The question remains as to which mechanism induces the efficiency of the photosynthetic apparatus in these plants.

Conclusions

Taken together, the transcriptome and metabolome data suggest the following hypothetical scenario (Figure 3). Downregulation of CAD and CCR reduces the flux of carbon towards lignin. This reduced flux is most pronounced for CCR-downregulated plants, which make significantly less lignin. The primary response of the partial block in these pathway steps is the accumulation of pathway intermediates and derivatives thereof, the disappearance of monolignol coupling products, and the alteration of cell-wall structure. The pathway intermediates repress gene expression in the phenylpropanoid pathway, possibly by feedback mechanisms. As a secondary response, the cell wall senses its altered structure and the need for further reinforcement of the wall with lignin. Therefore, starch is broken down to supply new monolignols for lignin, but because CAD and CCR are defective, the result is a further accumulation of pathway intermediates and a stronger repression of phenylpropanoid biosynthesis. The breakdown of starch and hemicellulose serves as the initial source of the glucose and quinate needed to detoxify and store the accumulating phenylpropanoid pathway intermediates (Figure 3).

A third event is the stress response that is most apparent in CCR-deficient lines. Possibly, plasma membrane-localized proteins sense the altered cell-wall structure and signal it to the nucleus, or the altered cell wall releases cell-wall fragments that act as elicitors to switch on gene expression. The increased photorespiration in CCR-deficient lines may as well be an important contributor to the oxidative stress.

Our data show that altering the expression of the late monolignol biosynthetic pathway genes *CCR* and *CAD* affects the transcript level of a high number of genes, revealing a substantial network of regulatory interactions both within monolignol biosynthesis, and among monolignol and other metabolic pathways. In the past, such effects were classified as pleiotropic and considered uninteresting because they could not be properly explained and linked with the gene under study. However, with the advent of transcript and metabolite profiling tools, the molecular details of these pleiotropic phenotypes can be revealed at

a much larger scale than before, and scenarios for how they relate to the modified gene can be proposed. Understanding these pleiotropic effects is important for several reasons. It provides new candidate genes that are closely related to the modified pathway. In addition, the genes of a given pathway for which transcript levels are affected might be those that regulate the flux through that pathway, and therefore correspond to interesting targets for pathway engineering.

Furthermore, knowing how the biosynthesis of the various cell-wall polymers is integrated, and how plants compensate for or respond to alterations in the biosynthesis of one of the wall polymers, is essential for designing cell walls for various end uses. Importantly, dissecting the complex pleiotropic phenotype at the molecular level might help in predicting the negative and unforeseen consequences of a mutation on plant health and quality. This knowledge opens up possibilities for mitigating these effects, for example by blocking adverse metabolic routes through genetic engineering or breeding. Our data also put the concept of substantial equivalence into perspective. Apparently, alterations in the expression of a single endogenous structural gene affect the expression of a plethora of other genes in various unanticipated pathways, putting into perspective concerns about unanticipated effects on metabolism caused by transgenes in genetically modified organisms.

Finally, our data reveal the amazing plasticity of the plant's metabolism in response to genetic variation. This metabolic plasticity, enabling plants to adapt to genetic variation, is probably important for plant populations to adapt to environmental conditions and must be considered essential for the long-term survival of populations (Booy *et al.*, 2000).

Experimental procedures

Tobacco lines

All tobacco plants used were *Nicotiana tabacum* L. cv. Samsun; wild-type plants are referred as WT. B3.1 and B6.8 are cinnamoyl CoA reductase (CCR) downregulated lines, homozygous for a construct containing a 1.3-kb fragment, corresponding to a full-length tobacco *CCR* cDNA, in the antisense orientation, coupled to the 35S CaMV promoter and the 3′ terminator of the nopaline synthase gene (Piquemal *et al.*, 1998). Seeds resulting from self-pollination of the homozygous line were used.

J48.7 and J40.31 are cinnamyl alcohol dehydrogenase (CAD) downregulated lines, homozygous for a construct containing a 1 kb fragment of the tobacco *CAD2* cDNA in the antisense orientation, coupled to the 35S CaMV promoter and the 3′ terminator of the nopaline synthase gene (Halpin *et al.*, 1994). Seeds resulting from self-pollination of the homozygous lines were used.

T16-1 T2F is a CAD-downregulated line, homozygous for an RNAi construct containing a 550 bp fragment of the 5′ region of tobacco *CAD2* in the sense and the antisense orientations flanking a 220 bp intron, coupled to the CaMV 35S promoter and 3′ terminator. The hemizygous lines resulting from the backcross of B3.1 and J48.7 with WT are B3 h and J48 h, respectively (Chabannes *et al.*, 2001a).

The double transformant Dt1a, obtained by crossing of the homozygous lines J48.7 x B3.1, is hemizygous for the two transgenes (Chabannes *et al.*, 2001a). Dt52.6 is a CCR- and CAD-downregulated line, homozygous for a chimeric construct with partial sense sequences of both *CAD* and *CCR* (Abbott *et al.*, 2002). All transgenic lines downregulated for CCR had slightly curled leaves that were a darker green than those of the WT. In addition, B3.1 and Dt52.6 developed yellowish areas between the leaf veins and were smaller than the other lines.

For convenience, throughout the text, 'asCCR' refers collectively to all *CCR* single-transformed lines described above, 'asCAD' to all *CAD* single-transformed lines described above, and 'DT' to the double transformants Dt1a and Dt52.6.

Growth and sampling conditions

Seeds of the various tobacco lines were surface-sterilized and germinated on solid Murashige and Skoog medium, grown under a light/dark regime of 16 h/8 h, 20–30 E m^{-2} sec^{-1}, at 27°C, and transferred after 4 weeks to soil and cultivated in a greenhouse (at 16 h/8 h and 25°C/22°C day/night).

For analyses of stem tissue (cDNA-AFLP, soluble phenolics, GC-MS, amino acid and pigment analyses), 10-week-old plants were harvested at 10 weeks old, just before flowering, and whole stems of WT and transgenic lines were frozen immediately in liquid nitrogen. All experiments were carried out on the basal half of the stem of the various tobacco lines. The cortex was removed, and the outer part of the woody ring was scraped off with a scalpel and ground for further analysis. For pigment analyses, the cortex was ground separately, and each sample of leaf tissue consisted of a pool of three 12 mm leaf discs, cut out of the 4th, 5th and 6th leaves, counting from the top. Samples were frozen in liquid nitrogen immediately upon harvest and were ground with metal balls in an MM300 high-frequency shaking instrument (Retsch); http://www.retsh.com). The following lines were used: in the cDNA-AFLP experiment, WT (n = 7) and the hemizygous downregulated lines B3 h (n = 7), J48 h (n = 7) and Dt1a (n = 7) for amino acid, soluble phenolics and GC-MS analyses, the lines B3.1 (n = 6), B6.8 (n = 6), J48.7 (n = 3), J40.31 (n = 3), Dt52.6 (n = 6), Dt1a (n = 6), T16-1 T2 F (n = 6) and WT (n = 12) for pigment analyses, the lines B3.1 (n = 5), B6.8 (n = 5), J48.7 (n = 3), J40.31 (n = 3), Dt52.6 (n = 5), Dt1a (n = 5) and WT (n = 5) for gas exchange analysis, WT (n = 16), and the lines B3.1 (n = 12) and Dt52.6 (n = 12) for chlorophyll fluorescence measurements in the light-acclimatized state, WT (n = 6), B3.1 (n = 6) and Dt52.6 (n = 6) and for chlorophyll fluorescence measurements in the dark-acclimatized state, WT (n = 29), B3.1 (n = 13), B6.8 (n = 13), J48.7 (n = 13), Dt52.6 (n = 13) and Dt1a (n = 13). Independently grown series of plants were utilized for (i) cDNA-AFLP, (ii) the amino acid, phenolic and GC-MS profiling, (iii) the pigment analysis and (iv) gas exchange and chlorophyll fluorescence measurements. Multiple lines were used to increase the robustness of the data. Statistical analysis revealed only those metabolites that were differential in all lines.

cDNA-AFLP analysis and data processing

For each genotype, two pools of xylem tissue, each from seven plants, were prepared for RNA extraction. Total RNA was prepared by the LiCl extraction method (Goormachtig *et al.*, 1995), from approximately 300 mg of pooled ground xylem. Using 5 μg of total RNA, cDNA-AFLP-based transcript profiling was performed essentially as described previously (Breyne *et al.*, 2002). The cDNAs were screened using all possible 128 MseI + 1/BstYI/

C + 2, 55 MseI + 2/BstYIT/C + 2 and six MseI+(2 or 3)/BstYIT/C+(2 or 3) primer combinations. Quantitative data were analysed using AFLP-QuantarPro software (Keygene; http://www.keygene.com). The exported normalized band intensity values were corrected for the lane intensity according to the method described by Breyne and Zabeau (2001). Bands with similar intensity in the two pools within each line, but different intensity in one or more transgenic lines, compared to WT, were selected first by visual scoring. From this selection, significant ($P < 0.05$) differential expression between the genotypes was determined for each transcript using one-way analysis of variance (ANOVA) with one fixed factor (genotypes) and the least significant difference (LSD) *post hoc* test (version 8; SAS Institute; http://www.sas.com). TDFs that, according to visual scoring and both statistical analyses, accumulated differentially between the WT and one or several other genotypes, were isolated from the gel, re-amplified and sequenced. Only when a sequence could be obtained directly from the re-amplified PCR product, or when, after cloning of this PCR product into the pGEM-T easy vector (Promega, http://www.promega.com/), individual clones gave one unambiguous sequence, was the corresponding intensity pattern on the gel assumed to be the result of a single transcript and was withheld as 'differential TDF' or dTDF. Sequences shorter than 21 nucleotides after removal of the primer sequence were not further considered. After log transformation and normalization of the mean expression data (with two replicates per genotype), the complete linkage hierarchical clustering algorithm and the tree-view algorithm (Eisen *et al.*, 1998) were used to group the dTDFs with similar behaviour in terms of transcript levels in the various transformants.

Homology search and identification of the transcript tags

The sequences obtained either from the re-amplified PCR product or from individual clones after cloning into pGEM-T easy (Promega) were compared by BLASTX (Altschul *et al.*, 1997) to a database containing all plant amino acid sequences from the Swiss-Prot and TrEMBL databases. If at least 10 amino acids were aligned in the best BLASTX hit, the alignment covered at least 80% of the overlap between the tag (query) and the sequence in the database (subject), and at least 50% of the amino acids in the alignment were identical between the query and the subject, the best BLASTX hit was accepted as homologue of the dTDF and its function assigned to the dTDF. If one or more of these parameters were not reached in the BLASTX output, BLASTN was performed on the transcript tag (Altschul *et al.*, 1997) against a database containing all EMBL and GenBank non-redundant plant nucleotide sequences, including expressed sequence tag and genome survey sequences. A BLASTN hit was accepted if an alignment of 30 bp or longer was obtained that covered at least 60% of the overlap, and if at least 80% of the base pairs within the alignment were identical between query and subject. If the alignment did not cover 60% of the overlap, a BLASTN hit was still accepted when at least 50 bp were aligned with at least 85% identity, or when at least 21 bp had a completely identical alignment, covering the complete overlap between the dTDF and the BLASTN hit. In this manner, TDFs that tend to be short and/or situated in the 3′ untranslated region could be replaced by longer EST or isolated cDNA sequences, increasing the chance of finding significant homology in a subsequent BLASTX.

The best BLASTX hit for each transcript was submitted to BLASTP against the protein sequences of the *Arabidopsis thaliana* database of the Institute for Genome Research. The Arabidopsis homologues of the differentially expressed transcripts were compared, at the amino acid level, to the differentially expressed genes in published Arabidopsis transcriptome analyses.

Metabolite profiling

Xylem was harvested and extracted as described previously (Damiani *et al.*, 2005; Morreel *et al.*, 2004a,b). Amino acid abundances were determined according to the method described by Rohde *et al.* (2004). Methanol-soluble phenolics were analysed by HPLC (Damiani *et al.*, 2005). Commercially available monolignol biosynthesis intermediates were spiked to identify their position on the chromatogram. Other HPLC peaks were identified using procedures described in Appendix S1. In addition, 802 derivatized polar metabolites, of which 159 are known metabolites, were revealed by GC-MS. Information on the polar metabolites, using the corresponding mass spectral identifiers (ID), may be found at http://csbdb.mpimp-golm.mpg.de/csbdb/gmd/msri/gmd_smq.html (Kopka *et al.*, 2005; Schauer *et al.*, 2005).

Chemicals

Sinapic acid and syringic acid were purchased from Janssen Chimica; http://www.fisher.co.uk), and quinic acid, ferulic acid, coniferaldehyde, sinapaldehyde, coniferyl alcohol and sinapyl alcohol were purchased from Sigma-Aldrich (http://www.sigmaaldrich.com/). The synthesis of feruloyl tyramine is an unpublished method available from J. Ralph and F. Lu (USDA, University of Wisconsin).

Quantitative analysis of pigments (chlorophylls a *and* b*, carotenoids and anthocyanins)*

Chlorophyll *a* (ChlA), chlorophyll *b* (ChlB), carotenoids and anthocyanins were quantified in xylem, cortex and leaf tissue. ChlA, ChlB and carotenoids were extracted by adding 500 μl of 80% acetone to the samples, centrifugation at 5000 ***g***, washing twice with 80% acetone, and centrifugation for 10 min at 5000 ***g***. Their absorption was measured using a SPECTRAmax™ 250 microplate spectrophotometer (Molecular Devices Corporation; http://www.moleculardevices.com) at 663, 646 and 470 nm. The concentrations of ChlA, ChlB and carotenoids were quantified according to the method described by Lichtenthaler and Wellburn (1983), as follows: ChlA (μg ml^{-1}) = 12.21 A_{663} – 2.81 A_{646}; ChlB (μg ml^{-1}) = 20.31 A_{646} – 5.03 A_{663}; carotenoids (μg ml^{-1}) = [1000 A_{470} – 1.82 ChlA (μg ml^{-1}) – 85.02 ChlB (μg ml^{-1})]/198.

Anthocyanins were extracted by adding 2 ml of 0.1% HCl in methanol to the sample, followed by 48 h of incubation at 4°C and centrifugation for 10 min at 5000 ***g***. By measuring the absorption at 530 and 675 nm, anthocyanins were quantified according to the method described by Rabino and Mancinelli (1986): anthocyanins = $A_{530} - (0.3 \times A_{657})$.

Statistical analysis of amino acids, pigments and soluble phenolics

The concentrations of the amino acids, pigments and the soluble phenolics were calculated per mg dry weight, and the data analysed statistically as described previously (Morreel *et al.*, 2004a,b). Briefly, significant differences ($\alpha_{model} = 0.05$; $\alpha_{line} = 0.01$; $\alpha_{enz} = 0.05$) were obtained by nested ANOVA model (1):

$$y_{ijk} = \mu + \text{enz}_i + \text{line}_{j(i)} + \varepsilon_{ijk} \quad (1)$$

where y_{ijk} is the value of the trait in individual *k* belonging to the *j*th tobacco line of the *i*th enzyme; μ is the overall mean trait value; enz_i and $line_{j(i)}$ are the deviations from the overall mean due to the effects of the downregulation of the *i*th enzyme and the *j*th tobacco line for the *i*th downregulated enzyme, respectively; and ϵ_{ijk} is the residual deviation of the trait value in individual *k* of the *j*th tobacco line for the *i*th downregulated enzyme. Box–Cox transformations were performed whenever necessary. If no homoscedasticity could be obtained for model (1), a one-way ANOVA was applied (α_{model}= 0.05). When appropriate, ANOVA was followed by an LSD *post hoc* test (α_{LSD} = 0.05).

Statistical analysis of GC-MS data

Data were analysed according to the method described by Damiani *et al.* (2005). Principal component analysis (PCA) of the GC-MS data revealed four main principal components (PC) that were able to separate the transgenic lines, explaining cumulatively 56.4% of the variance present in the dataset. Components that mainly contributed to these PC were determined when the absolute value of their loading factor was larger than 0.20 and larger than one standard deviation from the mean loading factor in that particular PC.

GC-MS profiles of WT, asCCR, asCAD and DT could be distinguished by PC_1, PC_3 and PC_4. PC_1 clustered asCAD partly independently from the other lines (see Figure S3). Nevertheless, values for asCAD were much more spread by PC_1 than for the other lines because downregulation was obtained with either RNAi or antisense T-DNA constructs. Those individual PC_1 values that afforded the partial separation all belonged to the more strongly RNAi downregulated CAD lines. PC_3 distinguished asCCR and DT lines from WT plants, whereas PC_4 separated asCCR lines from DT. Known metabolites that contributed predominantly to these PC and that were significantly differential based on a *t* test (α = 0.05), as well as those known metabolites that were only detected by a *t* test with a more stringent threshold (α = 0.001), are listed in Table 3.

Gas exchange and chlorophyll fluorescence analysis

Levels of photorespiration were determined from measurements of photosynthetic rates in air containing 21% O_2 and 2% O_2 using an infra-red CO_2 gas analyser LI-6400 (LI-COR; http://www.licor.com). Pre-mixed gases were supplied from pressurized tanks (Air America Liquide; http://www.airliquide.com). Measurements were made at saturating photon flux density (1200 μmol m^{-2} sec^{-1}), a leaf temperature of 25.5°C (SD = 0.7) and a vapour pressure deficit of 0.80 kPa (SD = 0.17).

A fluorescence chamber head (LI-6400-40; LI-COR) was integrated with the open gas exchange system LI-6400 to measure steady-state fluorescence (F_s), maximum fluorescence during a light saturating pulse (F'_m), and minimum fluorescence during far-red light illumination (F'_o). The photochemical quantum yield of electron transport through PSII was calculated as $\Phi_{PSII} = (F'_m - F'_s)/F'_m$ (Genty *et al.*, 1989). To account for the fact that PSII units are connected rather than independent, we used $qP = F'_o(F'_m - F_s)/F_s(F'_m - F'_o)$ as an estimate of the fraction of open PSII centers as proposed by Kramer *et al.* (2004). Because of the size of the LI-6400-40 leaf chamber fluorometer, it was not possible to avoid the lesions on the leaves of the CCR-downregulated tobacco plants.

F_v/F_m, i.e. the maximum quantum yield of primary photochemistry of PSII, was measured in the morning on dark-acclimatized (1 h) leaves using a 'plant efficiency analyser' (Hansatech; http://www.hansatech-instruments.com) as described previously (Gielen *et al.*, 2005). With this device, focus on the dark-green tissue was possible, thus avoiding the lesions. Photorespiration data and fluorescence measurements in the dark-acclimatized state were analysed by one-way ANOVA followed by an LSD *post hoc* test using SAS version 8.2 with the mixed procedure (Littell *et al.*, 1996). Because all data for asCCR and DT revealed similar differences and the fluorescence measurements obtained under light-acclimatized conditions were highly variable, the nested ANOVA model (2) was applied using *R*, version 2.4.1

$$y_{ijk} = \mu + tr_i + enz_{j(i)} + \varepsilon_{ijk} \quad (2)$$

where y_{ijk} is the value of the trait in individual *k* belonging to the *j*th line of the *i*th tobacco group (*I* = 0 or 1 for WT or transgenic tobacco), μ is the overall mean trait value, tr_i is the deviation from the overall mean due to the effects of CCR downregulation, $enz_{j(i)}$ expresses the particular deviation of either CCR or both CCR and CAD, and ϵ_{ijk} is the residual deviation of the trait value in individual *k*. A threshold level of 0.10 was used for all model parameters.

Acknowledgements

The authors thank Fachuang Lu for synthesizing the tyramine ferulate, Paul Schatz for providing the caffeoyl and feruloyl shikimic acids, Hoon Kim for oligolignol synthesis, Alexander Erban and Ines Fehrle for technical assistance with GC-MS metabolite profiling, and Martine De Cock for preparing the manuscript. This work was supported by the European Commission program (QLK5-CT-2000-01493; COPOL) and Research Foundation-Flanders (grant G.0352.05). R.D. is indebted to the Institute for the Promotion of Innovation by Science and Technology in Flanders for a pre-doctoral fellowship. B.G. and A.R. are Postdoctoral Researchers of the Research Foundation-Flanders.

Supplementary material

The following supplementary material is available for this article online:

Figure S1. Groups of similarly modulated dTDFs.

Figure S2. MS/MS spectra.

Figure S3. PCA plots.

Figure S4. H_2O_2 in tobacco leaves.

Table S1. dTDF identity and accumulation pattern.

Table S2. dTDFs belonging to the classes of unknown proteins, expressed proteins, hypothetical proteins and no hits.

Table S3. Differentially accumulating metabolites in asCCR, asCAD and DT as revealed by HPLC, and whose identity is still unknown.

Appendix S1. Additional methods.

This material is available as part of the online article from http://www.blackwell-synergy.com.

References

Abbott, J.C., Barakate, A., Pinçon, G., Legrand, M., Lapierre, C., Mila, I., Schuch, W. and Halpin, C. (2002) Simultaneous suppression of multiple genes by single transgenes. Down-regulation of three unrelated lignin biosynthetic genes in tobacco. *Plant Physiol.* **128**, 844–853.

Abdulrazzak, N., Pollet, B., Ehlting, J. *et al.* (2006) A *coumaroyl-ester-3-hydroxylase* insertion mutant reveals the existence of nonredundant *meta*-hydroxylation pathways and essential roles for phenolic precursors in cell expansion and plant growth. *Plant Physiol.* **140**, 30–48 [Erratum: *Plant Physiol.* 141, 1708].

Andersson Gunneråas, S. (2005) Wood formation and transcript analysis with focus on tension wood and ethylene biology. Doctoral thesis no. 2005–15. Umeå: Swedish University of Agricultural Sciences.

Altschul, S.F., Madden, T.L., Schäffer, A.A., Zhang, J., Zhang, Z., Miller, W. and Lipman, D.J. (1997) Gapped BLAST and PSI-BLAST: a new generation of protein database search programs. *Nucleic Acids Res.* **25**, 3389–3402.

Amthor, J.S. (2003) Efficiency of lignin biosynthesis: a quantitative analysis. *Ann. Bot.* **91**, 673–695.

Atanassova, R., Favet, N., Martz, F., Chabbert, B., Tollier, M.T., Monties, B., Fritig, B. and Legrand, M. (1995) Altered lignin composition in transgenic tobacco expressing *O*-methyltransferase sequences in sense and antisense orientation. *Plant J.* **8**, 465–477.

Baucher, M., Petit-Conil, M. and Boerjan, W. (2003) Lignin: genetic engineering and impact on pulping. *Crit. Rev. Biochem. Mol. Biol.* **38**, 305–350.

Besseau, S., Hoffmann, L., Geoffroy, P., Lapierre, C., Pollet, B. and Legrand, M. (2007) Flavonoid accumulation in *Arabidopsis* repressed in lignin synthesis affects auxin transport and plant growth. *Plant Cell*, **19**, 148–162.

Boerjan, W., Ralph, J. and Baucher, M. (2003) Lignin biosynthesis. *Annu. Rev. Plant Biol.* **54**, 519–546.

Booy, G., Hendriks, R.J.J., Smulders, M.J.M., Van Groenendael, J.M. and Vosman, B. (2000) Genetic diversity and the survival of populations. *Plant Biol.* **2**, 379–395.

Bray, E.A., Bailey-Serres, J. and Weretilnyk, E. (2000) Responses to abiotic stress. In *Biochemistry and Molecular Biology of Plants* (Buchanan, B.B., Gruissem, W. and Jones, R.L., eds). Rockville, MD: American Society of Plant Physiologists, pp. 1158–1203.

Breyne, P. and Zabeau, M. (2001) Genome-wide expression analysis of plant cell cycle modulated genes. *Curr. Opin. Plant Biol.* **4**, 136–142.

Breyne, P., Dreesen, R., Vandepoele, K. *et al.* (2002) Transcriptome analysis during cell division in plants. *Proc. Natl. Acad. Sci. USA* **99**, 14825–14830.

Bykova, N.V., Keerberg, O., Pärnik, T., Bauwe, H. and Gardeström, P. (2005) Interaction between photorespiration and respiration in transgenic potato with antisense reduction in glycine decarboxylase. *Planta*, **222**, 130–140.

Caño-Delgado, A., Penfield, S., Smith, C., Catley, M. and Bevan, M. (2003) Reduced cellulose synthesis invokes lignification and defense responses in *Arabidopsis thaliana*. *Plant J.* **34**, 351–362.

Chabannes, M., Barakate, A., Lapierre, C., Marita, J.M., Ralph, J., Pean, M., Danoun, S., Halpin, C., Grima-Pettenati, J. and Boudet, A.M. (2001a) Strong decrease in lignin content without significant alteration of plant development is induced by simultaneous down-regulation of cinnamoyl CoA reductase (CCR) and cinnamyl alcohol dehydrogenase (CAD) in tobacco plants. *Plant J.* **28**, 257–270.

Chabannes, M., Ruel, K., Yoshinaga, A., Chabbert, B., Jauneau, A., Joseleau, J.-P. and Boudet, A.-M. (2001b) *In situ* analysis of lignins in transgenic tobacco reveals a differential impact of individual transformations on the spatial patterns of lignin deposition at the cellular and subcellular levels. *Plant J.* **28**, 271–282.

Damiani, I., Morreel, K., Danoun, S. *et al.* (2005) Metabolite profiling reveals a role for atypical cinnamyl alcohol dehydrogenase CAD1 in the synthesis of coniferyl alcohol in tobacco xylem. *Plant Mol. Biol.* **59**, 753–769.

Dat, J.F., Pellinen, R., Beeckman, T., Van De Cotte, B., Langebartels, C., Kangasjärvi, J., Inzé, D. and Van Breusegem, F. (2003) Changes in hydrogen peroxide homeostasis trigger an active cell death process in tobacco. *Plant J.* **33**, 621–632.

Ehlting, J., Büttner, D., Wang, Q., Douglas, C.J., Somssich, I.E. and Kombrink, E. (1999) Three 4-coumarate:coenzyme A ligases in *Arabidopsis thaliana* represent two evolutionarily divergent classes in angiosperms. *Plant J.* **19**, 9–20.

Eisen, M.B., Spellman, P.T., Brown, P.O. and Botstein, D. (1998) Cluster analysis and display of genome-wide expression patterns. *Proc. Natl Acad. Sci. USA*, **95**, 14863–14868 [Erratum: *Proc. Natl Acad. Sci. USA*, 96, 10943].

Elkind, Y., Edwards, R., Mavandad, M., Hedrick, S.A., Ribak, O., Dixon, R.A. and Lamb, C.J. (1990) Abnormal plant development and down-regulation of phenylpropanoid biosynthesis in transgenic tobacco containing a heterologous phenylalanine ammonia-lyase gene. *Proc. Natl Acad. Sci. USA*, **87**, 9057–9061.

Ellis, C., Karafyllidis, I., Wasternack, C. and Turner, J.G. (2002) The Arabidopsis mutant *cev1* links cell wall signaling to jasmonate and ethylene responses. *Plant Cell*, **14**, 1557–1566.

Fukasawa-Akada, T., Kung, S.-d. and Watson, J.C. (1996) Phenylalanine ammonia-lyase gene structure, expression, and evolution in *Nicotiana*. *Plant Mol. Biol.* **30**, 711–722.

Genty, B., Briantais, J.-M. and Baker, N.R. (1989) The relationship between the quantum yield of photosynthetic electron transport and quenching of chlorophyll fluorescence. *Biochim. Biophys. Acta*, **990**, 87–92.

Gielen, B., De Boeck, H.J., Lemmens, C.M.H.M., Valcke, R., Nijs, I. and Ceulemans, R. (2005) Grassland species will not necessarily benefit from future elevated air temperatures: a chlorophyll fluorescence approach to study autumn physiology. *Physiol. Plant.* **125**, 52–63.

Goormachtig, S., Valerio-Lepiniec, M., Szczyglowski, K., Van Montagu, M., Holsters, M. and de Bruijn, F.J. (1995) Use of differential display to identify novel *Sesbania rostrata* genes enhanced by *Azorhizobium caulinodans* infection. *Mol. Plant–Microbe Interact.* **8**, 816–824.

Guillet, G. and De Luca, V. (2005) Wound-inducible biosynthesis of phytoalexin hydroxycinnamic acid amides of tyramine in tryptophan and tyrosine decarboxylase transgenic tobacco lines. *Plant Physiol.* **137**, 692–699.

Guo, D., Chen, F., Inoue, K., Blount, J.W. and Dixon, R.A. (2001) Downregulation of caffeic acid 3-*O*-methyltransferase and caffeoyl CoA 3-*O*-methyltransferase in transgenic alfalfa: impacts on lignin structure and implications for the biosynthesis of G and S lignin. *Plant Cell*, **13**, 73–88.

Halpin, C., Knight, M.E., Foxon, G.A., Campbell, M.M., Boudet, A.M., Boon, J.J., Chabbert, B., Tollier, M.-T. and Schuch, W. (1994) Manipulation of lignin quality by downregulation of cinnamyl alcohol dehydrogenase. *Plant J.* **6**, 339–350.

Harmer, S.L., Hogenesch, J.B., Straume, M., Chang, H.-S., Han, B., Zhu, T., Wang, X., Kreps, J.A. and Kay, S.A. (2000) Orchestrated transcription of key pathways in *Arabidopsis* by the circadian clock. *Science*, **290**, 2110–2113.

Henkes, S., Sonnewald, U., Badur, R., Flachmann, R. and Stitt, M. (2001) A small decrease of plastid transketolase activity in antisense tobacco transformants has dramatic effects on photosynthesis and phenylpropanoid metabolism. *Plant Cell*, **13**, 535–551.

Jaeck, E., Martz, F., Stiefel, V., Fritig, B. and Legrand, M. (1996) Expression of class I *O*-methyltransferase in healthy and TMV-infected tobacco. *Mol. Plant–Microbe Interact.* **9**, 681–688.

Jeong, M.L., Jiang, H., Chen, H.-S., Tsai, C.-J. and Harding, S.A. (2004) Metabolic profiling of the sink-to-source transition in developing leaves of quaking aspen. *Plant Physiol.* **136**, 3364–3375.

Kaplan, F., Kopka, J., Haskell, D.W., Zhao, W., Schiller, K.C., Gatzke, N., Sung, D.Y. and Guy, C.L. (2004) Exploring the temperature-stress metabolome of Arabidopsis. *Plant Physiol.* **136**, 4159–4168.

Knight, M.E., Halpin, C. and Schuch, W. (1992) Identification and characterisation of cDNA clones encoding cinnamyl alcohol dehydrogenase from tobacco. *Plant Mol. Biol.* **19**, 793–801.

Kopka, J., Schauer, N., Krueger, S. *et al.* (2005) GMD@CSB.DB: the Golm metabolome database. *Bioinformatics*, **21**, 1635–1638.

Kotake, T., Yamaguchi, D., Ohzono, H., Hojo, S., Kaneko, S., Ishida, H.-k. and Tsumuraya, Y. (2004) UDP-sugar pyrophosphorylase with broad substrate specificity toward various monosaccharide 1-phosphates from pea sprouts. *J. Biol. Chem.* **279**, 45728–45736.

Kozaki, A. and Takeba, G. (1996) Photorespiration protects C3 plants from photooxidation. *Nature*, **384**, 557–560.

Kramer, D.M., Johnson, G., Kiirats, O. and Edwards, G.E. (2004) New fluorescence parameters for determination of Q_A redox state and excitation energy fluxes. *Photosynth. Res.* **79**, 209–218.

Lee, D. and Douglas, C.J. (1996) Two divergent members of tobacco 4-coumarate: coenzyme A ligase (*4CL*) gene family. *Plant Physiol.* **112**, 193–205.

Lichtenthaler, H.K. and Wellburn, A.R. (1983) Determination of total carotenoids and chlorophylls *a* and *b* of leaf extracts in different solvents. *Biochem. Soc. Trans.* **11**, 591–592.

Lindahl, M., Tabak, S., Cseke, L., Pichersky, E., Andersson, B. and Adam, Z. (1996) Identification, characterization, and molecular cloning of a homologue of the bacterial FtsH protease in chloroplasts of higher plants. *J. Biol. Chem.* **271**, 29329–29334.

Littell, R.C., Milliken, G.A., Stroup, W.W. and Wolfinger, R.D. (1996) *SAS System for Mixed Models*. Cary, NC: SAS Institute Inc.

Loggini, B., Scartazza, A., Brugnoli, E. and Navari-Izzo, F. (1999) Antioxidative defense system, pigment composition, and photosynthetic efficiency in two wheat cultivars subjected to drought. *Plant Physiol.* **119**, 1091–1099.

Mellersh, D.G. and Heath, M.C. (2001) Plasma membrane–cell wall adhesion is required for expression of plant defense responses during fungal penetration. *Plant Cell*, **13**, 413–424.

Meyermans, H., Morreel, K., Lapierre, C. *et al.* (2000) Modification in lignin and accumulation of phenolic glucosides in poplar xylem upon down-regulation of caffeoyl-coenzyme A *O*-methyltransferase, an enzyme involved in lignin biosynthesis. *J. Biol. Chem.* **275**, 36899–36909.

Michal, G. (1999) *Biochemical Pathways: An Atlas of Biochemistry and Molecular Biology*. New York: John Wiley & Sons.

Möller, R. (2006) *Cell Wall Saccharification (Outputs from the Realising the Economic Potential of Sustainable Resources – Bioproducts from Non-food Crops (EPOBIO))*. Newbury, UK: CPL Press.

Morreel, K., Ralph, J., Kim, H., Lu, F., Goeminne, G., Ralph, S., Messens, E. and Boerjan, W. (2004a) Profiling of oligolignols reveals monolignol coupling conditions in lignifying poplar xylem. *Plant Physiol.* **136**, 3537–3549.

Morreel, K., Ralph, J., Lu, F., Goeminne, G., Busson, R., Herdewijn, P., Goeman, J.L., Van der Eycken, J., Boerjan, W. and Messens, E. (2004b) Phenolic profiling of caffeic acid *O*-methyltransferase-deficient poplar reveals novel benzodioxane oligolignols. *Plant Physiol.* **136**, 4023–4036.

Nagai, N., Kitauchi, F., Okamoto, K., Kanda, T., Shimosaka, M. and Okazaki, M. (1994) A transient increases in phenylalanine ammonia-lyase transcript in kinetin-treated tobacco callus. *Biosci. Biotechnol. Biochem.* **58**, 558–559.

Neill, S.O., Gould, K.S., Kilmartin, P.A., Mitchell, K.A. and Markham, K.R. (2002) Antioxidant activities of red versus green leaves in *Elatostema rugosum*. *Plant Cell Environ.* **25**, 539–547.

Nikiforova, V.J., Kopka, J., Tolstikov, V., Fiehn, O., Hopkins, L., Hawkesford, M.J., Hesse, H. and Hoefgen, R. (2005) Systems rebalancing of metabolism in response to sulfur deprivation, as revealed by metabolome analysis of Arabidopsis plants. *Plant Physiol.* **138**, 304–318.

Niyogi, K.K. (2000) Safety valves for photosynthesis. *Curr. Opin. Plant Biol.* **3**, 455–460.

O'Connell, A., Holt, K., Piquemal, J., Grima-Pettenati, J., Boudet, A., Pollet, B., Lapierre, C., Petit-Conil, M., Schuch, W. and Halpin, C. (2002) Improved paper pulp from plants with suppressed cinnamoyl-CoA reductase or cinnamyl alcohol dehydrogenase. *Transgenic Res.* **11**, 495–503.

Oliveira, I.C., Brears, T., Knight, T.J., Clark, A. and Coruzzi, G.M. (2002) Overexpression of cytosolic glutamine synthetase. Relation to nitrogen, light, and photorespiration. *Plant Physiol.* **129**, 1170–1180.

Panikulangara, T.J., Eggers-Schumacher, G., Wunderlich, M., Stransky, H. and Schöffl, F. (2004) *Galactinol synthase1*. A novel heat shock factor target gene responsible for heat-induced synthesis of raffinose family oligosaccharides in Arabidopsis. *Plant Physiol.* **136**, 3148–3158.

Pellegrini, L., Rohfritsch, O., Fritig, B. and Legrand, M. (1994) Phenylalanine ammonia-lyase in tobacco. Molecular cloning and gene expression during the hypersensitive reaction to tobacco mosaic virus and the response to a fungal elicitor. *Plant Physiol.* **106**, 877–886.

Piquemal, J., Lapierre, C., Myton, K., O'Connell, A., Schuch, W., Grima-Pettenati, J. and Boudet, A.-M. (1998) Down-regulation in cinnamoyl-CoA reductase induces significant changes of lignin profiles in transgenic tobacco plants. *Plant J.* **13**, 71–83.

Rabino, I. and Mancinelli, A.L. (1986) Light, temperature, and anthocyanin production. *Plant Physiol.* **81**, 922–924.

Raes, J., Rohde, A., Christensen, J.H., Van de Peer, Y. and Boerjan, W. (2003) Genome-wide characterization of the lignification toolbox in Arabidopsis. *Plant Physiol.* **133**, 1051–1071.

Ralph, J., Hatfield, R.D., Piquemal, J., Yahiaoui, N., Pean, M., Lapierre, C. and Boudet, A.M. (1998) NMR characterization of altered lignins extracted from tobacco plants down-regulated for lignification enzymes cinnamyl-alcohol dehydrogenase and cinnamoyl-CoA reductase. *Proc. Natl Acad. Sci. USA*, **95**, 12803–12808.

Ralph, J., Lundquist, K., Brunow, G. *et al.* (2004) Lignins: natural polymers from oxidative coupling of 4-hydroxyphenylpropanoids. *Phytochem. Rev.* **3**, 29–60.

Ranjan, P., Kao, Y.-Y., Jiang, H., Joshi, C.P., Harding, S.A. and Tsai, C.-J. (2004) Suppression subtractive hybridization-mediated transcriptome analysis from multiple tissues of aspen (*Populus tremuloides*) altered in phenylpropanoid metabolism. *Planta*, **219**, 694–704.

Robinson, A.R., Gheneim, R., Kozak, R.A., Ellis, D.D. and Mansfield, S.D. (2005) The potential of metabolite profiling as a selection tool for genotype discrimination in *Populus*. *J. Exp. Bot.* **56**, 2807–2819.

Roessner, U., Luedemann, A., Brust, D., Fiehn, O., Linke, T., Willmitzer, L. and Fernie, A.R. (2001) Metabolic profiling allows comprehensive phenotyping of genetically or environmentally modified plant systems. *Plant Cell*, **13**, 11–29.

Rogers, L.A., Dubos, C., Cullis, I.F., Surman, C., Poole, M., Willment, J., Mansfield, S.D. and Campbell, M.M. (2005) Light, the circadian clock, and sugar perception in the control of lignin biosynthesis. *J. Exp. Bot.* **56**, 1651–1663.

Rohde, A., Morreel, K., Ralph, J. *et al.* (2004) Molecular phenotyping of the *pal1* and *pal2* mutants of *Arabidopsis*

thaliana reveals far-reaching consequences on phenylpropanoid, amino acid, and carbohydrate metabolism. *Plant Cell*, **16**, 2749–2771.

Schauer, N., Steinhauser, D., Strelkov, S. *et al.* (2005) GC-MS libraries for the rapid identification of metabolites in complex biological samples. *FEBS Lett.* **579**, 1332–1337.

Shi, C., Koch, G., Ouzunova, M., Wenzel, G., Zein, I. and Lübberstedt, T. (2006) Comparison of maize brown-midrib isogenic lines by cellular UV-microspectrophotometry and comparative transcript profiling. *Plant Mol. Biol.* **62**, 697–714.

Sibout, R., Eudes, A., Mouille, G., Pollet, B., Lapierre, C., Jouanin, L. and Séguin, A. (2005) *CINNAMYL ALCOHOL DEHYDROGENASE-C* and *-D* are the primary genes involved in lignin biosynthesis in the floral stem of Arabidopsis. *Plant Cell*, **17**, 2059–2076.

Sundberg, B., Uggla, C. and Tuominen, H. (2000) Cambial growth and auxin gradients. In *Cambium: The Biology of Wood Formation* (Savidge, R., Barnett, J. and Napier, R., eds). Oxford: BIOS Scientific Publishers, pp. 169–188.

Tamagnone, L., Merida, A., Parr, A., Mackay, S., Culianez-Macia, F.A., Roberts, K. and Martin, C. (1998a) The AmMYB308 and AmMYB330 transcription factors from Antirrhinum regulate phenylpropanoid and lignin biosynthesis in transgenic tobacco. *Plant Cell*, **10**, 135–154.

Tamagnone, L., Merida, A., Stacey, N., Plaskitt, K., Parr, A., Chang, C.-F., Lynn, D., Dow, J.M., Roberts, K. and Martin, C. (1998b) Inhibition of phenolic acid metabolism results in precocious cell death and altered cell morphology in leaves of transgenic tobacco plants. *Plant Cell*, **10**, 1801–1816.

US Department of Energy (2006) *Breaking the Biological Barriers to Cellulosic Ethanol: A Joint Research Agenda, DOE/SC-0095*. Washington, DC: US Department of Energy Office of Science and Office of Energy Efficiency and Renewable Energy, pp. 39–56.

van Heerden, P.S., Towers, G.H.N. and Lewis, N.G. (1996) Nitrogen metabolism in lignifying *Pinus taeda* cell cultures. *J. Biol. Chem.* **271**, 12350–12355.

Vandenabeele, S., Vanderauwera, S., Vuylsteke, M., Rombauts, S., Langebartels, C., Seidlitz, H.K., Zabeau, M., Van Montagu, M., Inzé, D. and Van Breusegem, F. (2004) Catalase deficiency drastically affects gene expression induced by high light in *Arabidopsis thaliana*. *Plant J.* **39**, 45–58.

Vanderauwera, S., Zimmermann, P., Rombauts, S., Vandenabeele, S., Langebartels, C., Gruissem, W., Inzé, D. and Van Breusegem, F. (2005) Genome-wide analysis of hydrogen peroxide-regulated gene expression in Arabidopsis reveals a high light-induced transcriptional cluster involved in anthocyanin biosynthesis. *Plant Physiol.* **139**, 806–821.

Wingler, A. (2002) The function of trehalose biosynthesis in plants. *Phytochemistry*, **60**, 437–440.

Zhu, J.-K., Damsz, B., Kononowicz, A.K., Bressan, R.A. and Hasegawa, P.M. (1994) A higher plant extracellular vitronectin-like adhesion protein is related to the translational elongation factor-1α. *Plant Cell*, **6**, 393–404.

